Supporting Information for:

Upcycling Single-Use Polyethylene into High-Quality Liquid Products

Gokhan Celik,[1] Robert M. Kennedy,[1] Ryan A. Hackler,[1] Magali Ferrandon,[1] Akalanka Tennakoon,[2,3] Smita Patnaik,[2,3] Anne M. LaPointe,[4] Salai C. Ammal,[5] Andreas Heyden,[5] Frédéric A. Perras,[2] Marek Pruski,[2,3] Susannah L. Scott,[6] Kenneth R. Poeppelmeier,[7]* Aaron D. Sadow,[2,3]* Massimiliano Delferro[1]*

[1]Chemical Sciences and Engineering Division, Argonne National Laboratory, Lemont, IL 60439, USA

[2]U.S. DOE Ames Laboratory, Ames, IA 50011, USA

[3]Department of Chemistry, Iowa State University, Ames, IA 50011, USA

[4]Department of Chemistry and Chemical Biology, Cornell University, Ithaca, NY 14583, USA

[5]Department of Chemical Engineering, University of South Carolina, Columbia, SC 29208, USA

[6]Department of Chemical Engineering, University of California, Santa Barbara, CA 93106, USA

[7]Department of Chemistry, Northwestern University, Evanston, IL 60208, USA

Table of Contents

S1. General Procedures

Safety Statement: No unexpected or unusually high safety hazards were encountered.

A. Catalyst Synthesis and Materials

i. Strontium Titanate ($SrTiO_3$) Synthesis

$SrTiO_3$ nanocuboids were synthesized hydrothermally, following our previously published procedure.[S1] Glacial acetic acid (>99), strontium hydroxide octahydrate (99.995% trace metals basis), anhydrous ethanol (99.5%), titanium tetrachloride (99.9% trace metals basis), and sodium hydroxide pellets (99.99% trace metals basis) were purchased from Sigma Aldrich and used without additional purification. Strontium hydroxide and sodium hydroxide were stored in a vacuum desiccator. Ethanol and titanium tetrachloride were stored in a glove box under nitrogen. The acidic titanium tetraethoxy ethanol solution was prepared in the glove box and transferred to a fume hood after the solution had ceased fuming. Mixing the titanium tetrachloride and ethanol under nitrogen minimized unwanted side reactions with water or oxygen, observable by a dark orange color in the solution. The solutions were heated in Parr autoclaves to 240 °C at 1 °C/minute and held at that temperature for 36 hours before cooling to room temperature.

ii. $Pt/SrTiO_3$ Synthesis by Atomic Layer Deposition

Platinum nanoparticles (NPs) were deposited onto the $SrTiO_3$ nanocuboid supports using atomic layer deposition in a viscous flow reactor, adapted from previously described methods.[S2] Trimethyl(methylcyclopentadienyl)platinum(IV) ((MeCp)$PtMe_3$, Strem Chemicals, 99%) and 70% output O_3 (Pacific Ozone L11 Ozone Generator, ultra-high purity (UHP) 20 Torr O_2 source) was used with 300 s static doses of each precursor with 300 s N_2-assisted purge steps. Reactor temperature was set to 200 °C with the Pt bubbler set to 65 °C and Pt line set to 80 °C. A pre-treatment of O_3 exposure at 200 °C for 2 h was used for all ALD-prepared Pt samples. A various number of ALD cycles were used to prepare Pt NPs of various sizes, ranging from 1 to 10 ALD cycles. The ozone pre-treatment used should produce a suitable amount of nucleation sites for Pt ALD and remove possible carbonates on the surface.[S3, S4]

iii. Commercial Catalysts and PE Substrates

Pt/Al_2O_3 (1 wt% Pt, Sigma Aldrich) and γ-Al_2O_3 (Strem Chemicals) catalysts were obtained commercially. Pt/Al_2O_3 was ground to obtain fine powder samples. γ-Al_2O_3 was used as received.

PE substrates were purchased from Sigma-Aldrich (Product number = 427799) and Scientific Polymer Products, Inc (Product number: 562, 1018, and 565). The plastic bag was obtained from Aspen-Can Liners, North American Corporation (Product number: 380414). The molecular weight and degree of branching of the PE substrates are presented in Table S6.

iv. ^{13}C-labeled Polyethylene Synthesis

Ethylene-^{13}C (99% enriched 1,2-$^{13}C_2$) was obtained from Cambridge Isotope Lab in a 250 mL glass vessel and used without purification. Methylaluminoxane (MAO) was obtained from Sigma-Aldrich as a 10 wt % in toluene solution; toluene was evaporated, and the white solid material was washed with pentane (5 × 10 mL) to give a shiny white solid after exhaustive drying. The titanium polymerization catalyst containing a bulkier phenoxyimine chelating ligand was synthesized following literature procedure.[S5]

^{13}C-labeled polyethylene was prepared by the following procedure: A Schlenk round bottom flask was charged with a toluene solution (50 mL) of MAO (0.044 g, 0.74 mmol). 1,2-$^{13}C_2H_4$ (250 mL) was condensed into the reaction vessel cooled in a liquid nitrogen bath. The vessel was sealed and allowed to warm to room temperature, and then the mixture was cooled to 0 °C. The Ti-phenoxyimine catalyst (0.002 g, 0.002 mmol), dissolved in a minimal amount of toluene, was added to the reaction mixture through a septum. The resulting solution was stirred at 0 °C for 10 min and then allowed to warm to room temperature. Stirring was continued for 30 min at room temperature. The solution was then poured into a 5% HCl in MeOH solution to precipitate the polymer. The precipitate was isolated by filtration and dried under reduced pressure to yield ^{13}C-labeled polyethylene as a white solid (0.43 g). The polymer was characterized by HT GPC (M_n = 132,000 kg/mol; M_w = 429,800; $Đ$ = 3.2).

^{13}C-labeled polyethylene was adsorbed onto the surface of the support by the following procedure: ^{13}C-labeled polyethylene (12 mg) and the appropriate support (100 mg) were mixed in 1,2-dichlorobenzene (5 mL). This suspension was heated to 130 °C for 6 h. The liquid was separated from the solid by decanting while hot (~130 °C), and the solid was washed with hot (~130 °C) 1,2-dichlorobenzene (3 ×10 mL). The material was dried under vacuum at 120 °C for 12 h.

B. Characterization Techniques

i. Electron Microscopy (EM)

The size and morphology of the $SrTiO_3$ nanocuboids were characterized by electron microscopy, using a Hitachi HD-2300A Dual EDS scanning transmission electron microscope (STEM) at 200 kV in the BioCryo facility at Northwestern University's NUANCE Center. The diameter and interparticle spacing of Pt NPs on the $SrTiO_3$ and γ-Al_2O_3 supports were characterized using the JEOL ARM200CF aberration-corrected transmission electron microscope (TEM) at 200 kV in the EPIC facility at the NUANCE center and the FEI Talos STEM at 200 kV in the Center for Nanoscale Materials at Argonne National Laboratory. Annular bright field (ABF) and high angle annual dark field (HAADF) images were used to measure the face-to-face distance of $SrTiO_3$ nanocuboids and the diameters and positions in the imaging plane of platinum nanoparticles. To

determine the interparticle distances of Pt nanoparticles on the (100) facets of $SrTiO_3$, the cuboids were oriented so that the beam was oriented along a {100} zone axis. In this condition, the $SrTiO_3$ (100) facet under observation and the Pt NPs on its surface are parallel to the imaging plane and there is minimal geometric divergence. This allows the interparticle distances to be measured directly from the XY coordinates in the micrographs. As there is more variation in the topology of the alumina support, an interparticle distance was not determined from the electron micrographs.

The particle measurements were made using the FIJI[S6] distribution of ImageJ2.[S7] Digital Micrograph 4 (dm4) files were imported using the Bio-Formats plugin[S8] and FEI micrograph files were imported using the TIA Reader plugin by Steffen Schmidt. The Feret's diameter was measured using the built-in ellipsoid tool in ImageJ for 1) the $SrTiO_3$(100) facet-facet distance for cuboids and 2) the maximum diameter for Pt NPs. For the Pt NPs, the centroid of the ellipse was used as the center position of the particle for calculating the interparticle distance.

The average diameter and interparticle distances were calculated using Python scripts written in Jupyter Notebook,[S9] with the NumPy[S10] and Matplotlib[S11] packages. The average interparticle distance was calculated as the average of the first three nearest neighbor distances for every platinum particle on the (100) facet, excluding any distances that were longer or shorter than 1.5 times the interquartile range (IQR) as outliers (i.e. an isolated Pt NP that was measured for its diameter but was not near any other measured Pt NPs). Over 100 $SrTiO_3$ nanocuboids or Pt nanoparticles were used in calculating the diameters and interparticle distances in each calculation.

ii. Inductively-Coupled Plasma (ICP) – Optical Emission Spectrometry (OES):

Metal analysis was performed at the Northwestern University Quantitative Bio-element Imaging Center. Quantification of Pt, Sr and Ti was accomplished using ICP-OES of acid digested samples. Specifically, solid samples were digested in concentrated trace nitric acid (> 69%, Thermo Fisher Scientific, Waltham, MA, USA) and concentrated hydrochloric acid (> 34%, Thermo Fisher Scientific, Waltham, MA, USA) and placed at 65 °C for at least 3 hours. To the resulting mixture, 10 drops of 5% hydrofluoric acid (diluted from > 47% hydrofluoric acid, VWR International, Radnor, PA, USA) was added and samples were left at room temperature for 12 hours to allow for complete sample digestion. Ultra-pure H_2O (18.2 MΩ·cm) was added to produce a final solution of 2.0% nitric acid (v/v) and 2.0% hydrochloric acid (v/v) in a total sample volume of 10 mL. Dilutions of these samples were prepared by diluting 1 mL of stock sample solution with 9 mL of 2.0% nitric acid (v/v) and 2.0% hydrochloric acid (v/v). Quantitative standards consisting of 40/40/25, 20/20/12.5, 10/10/6.25, 5/5/3.125, 2.5/2.5/1.5625, and 1.25/1.25/0.78125 ng/g Ti/Sr/Pt were made using a 1000 µg/mL Pt standard, a 100 ug/mL Sr standard, and a 100 ug/mL Ti standard (Inorganic Ventures, Christiansburg, VA, USA) in 2.0% nitric acid (v/v) and 2.0% hydrochloric acid (v/v) in a total sample volume of 5 mL.

ICP-OES was performed on a computer-controlled (QTEGRA software) Thermo iCap7600 ICP-OES (Thermo Fisher Scientific, Waltham, MA, USA) operating in radial view and equipped with a CETAC 520 autosampler (Omaha, NE, USA). Each sample was acquired using 5 second visible

exposure time and 15 second UV exposure time, running 3 replicates. The spectral lines selected for analysis were: Ti (334.941, 323.452, and 337.280 nm), Pt (214.423, 214.423, and 214.423 nm) and Sr (407.771, 421.552, and 346.446 nm).

iii. Solid-state Nuclear Magnetic Resonance (ssNMR)

Solid-state nuclear magnetic resonance (ssNMR) experiments were performed using a Varian 600 MHz NMR system equipped with a 3.2-mm MAS probe. Samples were tightly-packed into 3.2-mm pencil-type rotors and spun to 16 kHz. Quantitative MAS spectra were acquired with a Bloch decay experiment using a 5 μs ^{13}C excitation pulse and a 10 s recycle delay. A total of 128, 3072, 8192, and 1024 scans were accumulated for the $SrTiO_3$, $Pt/SrTiO_3$, Al_2O_3, and Pt/Al_2O_3 samples, respectively. The ^{13}C CPMAS spectra were acquired using a 3.2 μs ^{1}H excitation pulse, a 1 ms contact time, and a recycle delay of 5 s. A total of 128 scans were accumulated for both $SrTiO_3$ samples and 32768 and 2047 scans were accumulated for the Al_2O_3 and Pt/Al_2O_3 samples, respectively. 80 kHz SPINAL-64 ^{1}H decoupling was used in during the acquisition of all spectra.

C. Chromatography Analysis and Nuclear Magnetic Resonance

i. Gas Chromatography (GC)

Gas samples taken from the headspace of the Parr reactor were analyzed on-line by the gas chromatograph (Agilent 6890N) equipped with automated sampling valves, a capillary column (Agilent, HP-Plot Al_2O_3-S, 25 m x 0.320mm x 8.0 micron), and a flame ionization detector. The GC was calibrated for C_1-C_8 saturated alkanes to obtain retention times and response factors. For the gas-phase distribution, detection of higher hydrocarbons than C_8 was limited by the separation achieved in the GC column.

ii. Double Shot Pyrolysis Gas Chromatography-Mass Spectrometry (GC-MS)

Experiments were performed on a Frontier EGA/PY-3030D attached to an Agilent 6890 GC exact mass spectrometer. For each experiment, 100-250 μg of polymer sample was loaded into a crucible, which was lowered into the furnace of the pyrolyzer. The sample was evacuated to 10-6 mTorr, and then heated from 40 to 400 °C at a ramp rate of 20 °C/min. Thermally desorbed (TD) components from the samples at these temperatures were cryo-trapped at –196 °C using a liquid nitrogen-cooled trap. When the furnace temperature reached 400 °C, the cryo-trapped components were injected into the GC for separation (Restek DB-5-HT column, ramped from 40 to 320 °C at 10 °C/min) and analysis through MS. Then, the furnace of the pyrolyzer was heated to 600 °C to pyrolyze the remaining sample into volatile components, which were subsequently analyzed by GC-MS.

iii. High Temperature Gas Permeation Chromatography (HT GPC)

Molecular weights (M_n and M_w) and molecular weight distributions ($Đ = M_w/M_n$) of polymers were determined by size exclusion chromatography (SEC) using monodisperse polyethylene standards. Analyses were performed using an Agilent PL-GPC-220 equipped with a refractive index (RI) detector. The column set (three Agilent PL-Gel Mixed B columns and one PL-Gel Mixed B guard column) was operated with 1,2,4-trichlorobenzene containing 0.01 wt% 3,5-di-tert-butyl-4-

hydroxytoluene (BHT) at a flow rate of 1.0 mL/min at 150 °C. The samples were prepared in TCB (with BHT) at a concentration of 1.0 mg/mL unless otherwise stated and heated at 150 °C for at least 1 hour prior to injection. GPC data calibration was done with monomodal polyethylene standards from Agilent and Polymer Standards Service, Inc.

The accuracy of the GPC to determine M_w and M_n below M_n = 1,000 Da was important to these studies. The GPC was calibrated with a set of linear monodisperse PE standards, including a standard with M_p = 500 Da. To further verify the accuracy at low molecular weights, linear alkane and alkene samples (n-eicosene, n-triacontane, *n*-hexatriacontane, and Unilyn1000, a hydroxyl terminated PE with M_w approximately 1000 Da) were analyzed alone and in mixtures. The linear hydrocarbons showed narrow dispersities (M_w/M_n = 1.01) and exhibited a good agreement between actual molecular weight and M_n (observed). Good separation could be observed between the M_w = 1,000 sample and the M_w = 300-500 samples. For this reason, we are confident that we are accurately determining molecular weight distributions between 400 and 1000 Da. The comparisons are listed below in Table S1.

Table S1. GPC analyses of several standard linear alkanes and alkenes

Sample	Actual	Mn	Mw	Mw/Mn
$C_{36}H_{74}$	**506**	**536**	**540**	**1.01**
$C_{20}H_{40}$	**280**	**311**	**314**	**1.01**
$C_{30}H_{62}$	**422**	**455**	**458**	**1.01**
Unilyn 1000	**1000**	**921**	**1048**	**1.14**

iv. Solution Phase ^{1}H and ^{13}C Nuclear Magnetic Resonance

Solution NMR experiments were conducted using a Bruker UltraShield 500 MHz spectrometer (^{1}H = 500 MHz, ^{13}C = 125 MHz) and the spectra were analyzed using MestReNova (v11.0.1, Mestrelab Research S.L.). Chemical shifts (δ) for ^{1}H and ^{13}C are referenced to tetramethylsilane (TMS), internal solvent resonances relative to TMS, and the polymer CH_2 backbone. NMR analysis of wax product was carried out in 1,2-dichlorobenzene-d4 at 25 °C with d1 = 10s and referenced to the polymer CH_2 backbone.

Long-chain branching density of PE substrates and the high-quality liquid product (M_n = 1,200 Da) obtained with 5c-Pt/$SrTiO_3$ catalyst after 68 hs was determined by ^{1}H NMR using the following formula: branches per 1000 carbons = $(CH_3/3)/\{(CH + CH_2 + CH_3)/2\}$ x 1000. CH_3, CH_2, and CH refer to the integrations obtained for the methyl, methylene, and methine resonances, respectively.[S12, S13]

D. Computational Details

i. Density Functional Theory (DFT) Calculations

DFT calculations were performed using the Vienna *ab initio* simulation package (VASP).[S14-17] The projector augmented wave (PAW)[S18,S19] method was used to describe the electron-ion interaction, whereas the exchange-correlation effects were included by means of the "strongly constrained and appropriately normed" (SCAN)[S20] meta-generalized gradient approximation functional. The SCAN functional is further paired with the *r*VV10 nonlocal density functional[S21] in order to properly account for the intermediate and long-range van der Waals interactions during hydrocarbon adsorption. Plane-waves were expanded using an energy cutoff of 500 eV. Four-layer slabs were used to model the Pt(100) and Pt(111) surfaces and the bottom two layers of the slabs were fixed at their bulk positions during structural optimization. A (6×4) surface unit cell with a (3×2×1) k-point mesh based on Monkhorst-Pack scheme[S22] and a $(3\sqrt{2}\times\sqrt{6})$ surface unit cell with a (2×3×1) k-point mesh were used for the Pt(100) and Pt(111) surface models, respectively. Dipole and quadrupole corrections to the energy were taken into account using a modified version of the Makov and Payne method[S23] and Harris-Foulke-type corrections[S24] were included for the forces.

The TiO_2 double-layer terminated $SrTiO_3$ surface was constructed using the following procedure. We initially built a (3×3) surface unit cell of a TiO_2-terminated $SrTiO_3$(001) surface with seven atomic layers separated by a vacuum spacing of 20 Å. The bottom three layers of the slab were maintained in their bulk parameters and the upper four layers were relaxed during structural optimization. The TiO_2 overlayer was then constructed based on the (3×3) surface reconstruction determined from combined transition electron diffraction and DFT studies.[S25] This structure was found to be consistent with experimental STM images[S26] and the surface energy of this structure was found to be very close to the lowest-energy configuration, $(\sqrt{13}\times\sqrt{13})$R33.7° identified by Kienzle et. al.[S25] The optimized unit cell with the TiO_2 overlayer was further expanded to a (6×3) surface unit cell and a (1×2×1) k-point mesh was used to examine hydrocarbon adsorption.

ii. Numerical Hydrogenolysis Modeling

Numerical catalytic hydrogenolysis models were used to compare the effects on the overall molecular weight distribution of different possible interactions of polyethylene with the catalyst. A population of linear alkanes is used, with a distribution corresponding to the GPC-measured molecular weights of the Sigma-Aldrich sourced PE used elsewhere in this study. The polyethylene is cleaved by a single catalytic site that hydrogenolyzes at a constant rate (Figure S6). The changes in the molecular weight (number and weight averaged) and dispersity are monitored with time. The models were calculated using Python scripts written in Jupyter Notebook,[S9] with the NumPy[S10] and Matplotlib[S11] packages.

When a molecule is "hydrogenolyzed" by the catalyst, it is removed from the population, cleaved at a random point between two carbons, and two new molecules corresponding to the products are added back into the population. For both models, if after being chopped, one or both of the products has eight or fewer carbons, they are removed from the population, as they would 1) be in the gas

phase during the reaction and have a lower probability of interacting with the catalyst than alkanes still in the melt, and 2) would not be measured by GPC. In the "random" model (Figure S6a), the probability of a molecule being hydrogenolyzed is equal, representing an equal probability of any molecule adsorbing on the catalyst. The "weighted" model (Figure S6b) represents the case when the strength of adsorption of an alkane on the catalyst increasing linearly with the number of carbons, as predicted by DFT.

E. Catalytic Activity Testing

i. Parr Reactor:

A Parr autoclave reactor with a mechanical stirrer was used for PE hydrogenolysis experiments. A quartz liner filled with 3 g of PE and a pre-determined amount of catalyst was placed in the reactor. Then, the reactor was sealed, tightened, and placed in the reactor assembly. Before starting the reaction, the lines and the reactor were flushed with helium to eliminate the presence of oxygen. Once the flushing was over, stirring was started and the temperature was increased to 300 °C at a ramp rate of 10 °C/min. The reactor was stirred at 1700 rpm to ensure well mixing and to minimize mass transfer limitations. Once the temperature was stabilized, hydrogen at 170 psi was introduced to the reactor and the reaction was started. At the end of the reaction, mixing was stopped, and a gas sample was immediately taken using a sample loop having a two-valve system. The gas in the sample loop was then introduced online to a gas chromatograph to determine the concentration of light hydrocarbons. In hydrogenolysis experiments, pressure increase was noted and taken into consideration to calculate the number of moles of light hydrocarbons (C_1-C_8) formed using ideal-gas law.

To assess the catalyst activity and properties of the Pt sites of the post-reaction catalysts, the reaction medium was physically recovered after 18 h-long catalytic activity experiments and subjected to Soxhlet extraction using hexane as a solvent.

ii. High-Throughput Testing

A Screening Pressure Reactor (SPR, Unchained Labs Inc.) at the Argonne National Laboratory's High-throughput Research Facility, was used for the high-throughput experiments. The SPR, is designed to carry out pressure reactions with heating and orbital shaking. Protocols were designed in Library Studio while Automation Studio (LEA software) was used for running the protocols. Simultaneous testing of all the catalysts and controls were carried out in multi-well plates that can hold 48 2-mL glass vials per run. Various amounts of catalysts were loaded in 0.5 dr. shell vials with various amounts of polymer which were loaded into the multi-well plate. The plate was then transferred into a clam-shell reactor, which was sealed and taken out to the SPR station. Initially, the SPR was set to shake at 300 rpm, flushed with 500 mL/min N_2 (UHP grade) for 15 min, then H_2 (UHP grade) for 15 min at room temperature. The reactor was then pressurized with H_2 and then heated up slowly (1 ºC/min ramp rate) to the desired temperature (100 to 350 °C). Under the given conditions, the pressure of the reactor was increased to reached 100-600 psig. After 1-96h, the shaking was stopped, the reactor was cooled down to room temperature, and was flushed with

100 mL/min N_2 (UHP) for 15 min. Samples were retrieved and sent for GPC analyses. Yield, presented in Table 1, was calculated as the percentage weight of the hydrogenolyzed liquid product at the end of the reaction divided by starting amount of PE. The weight changes of catalyst samples were not taken into consideration in this calculation.

S2. Supplementary Data

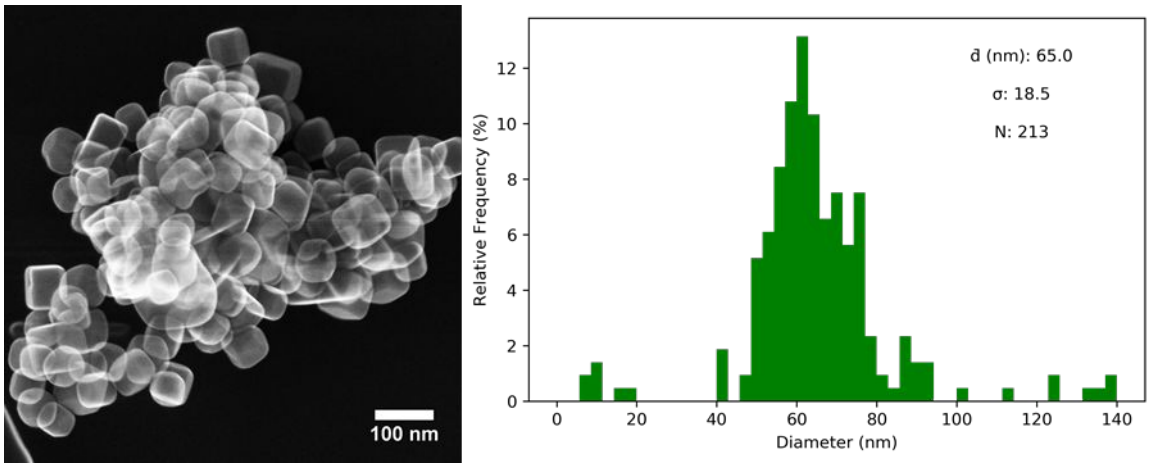

Figure S1. Electron micrograph of $SrTiO_3$ nanocuboid supports with a histogram showing the particle size distribution.

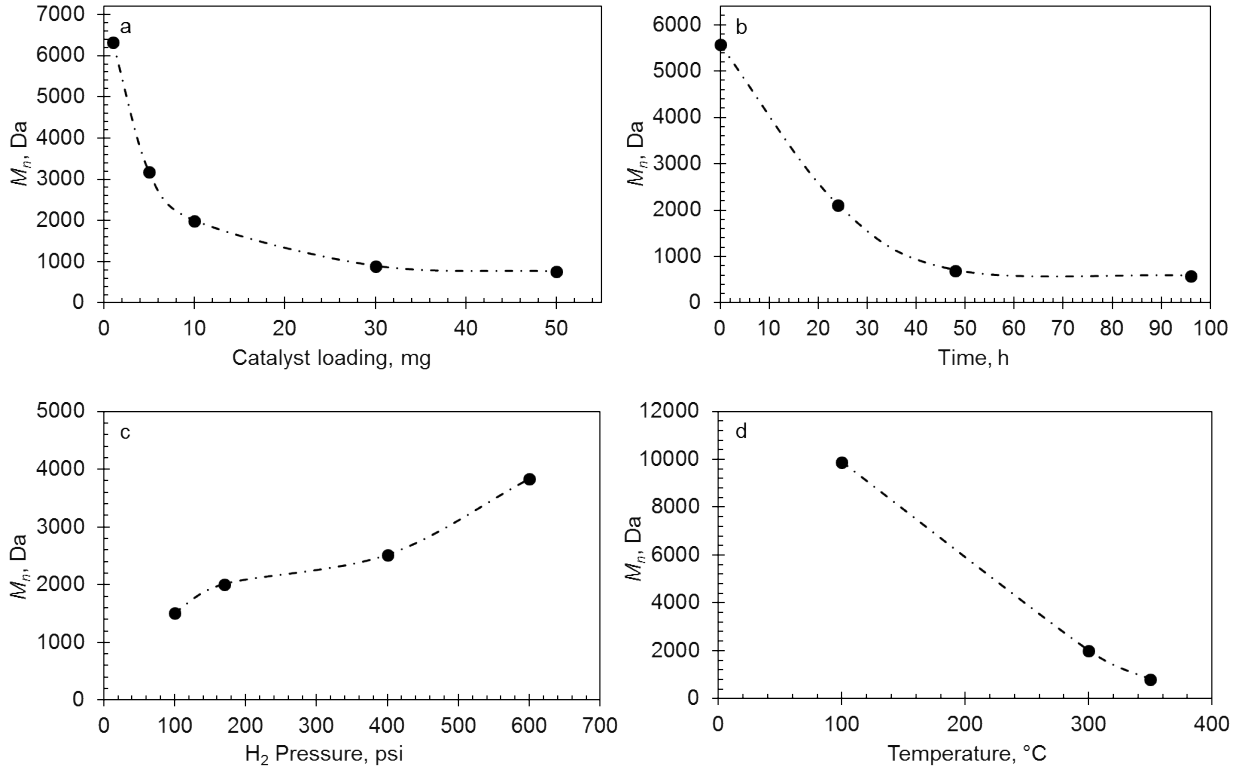

Figure S2. High-throughput hydrogenolysis of PE (M_n = 8,150 Da) experiments using the screening pressure reactor (SPR) over 5c-Pt/$SrTiO_3$. (a) effect of catalyst loading, (b) effect of reaction time, (c) H_2 pressure, and (d) temperature on M_n. Unless otherwise mentioned, reaction conditions are as the followings: catalyst amount = 0.14 mg Pt as 5c-Pt/$SrTiO_3$ (1.4% wt% Pt), time = 24 h, H_2 pressure = 170 psi, and temperature = 300 °C.

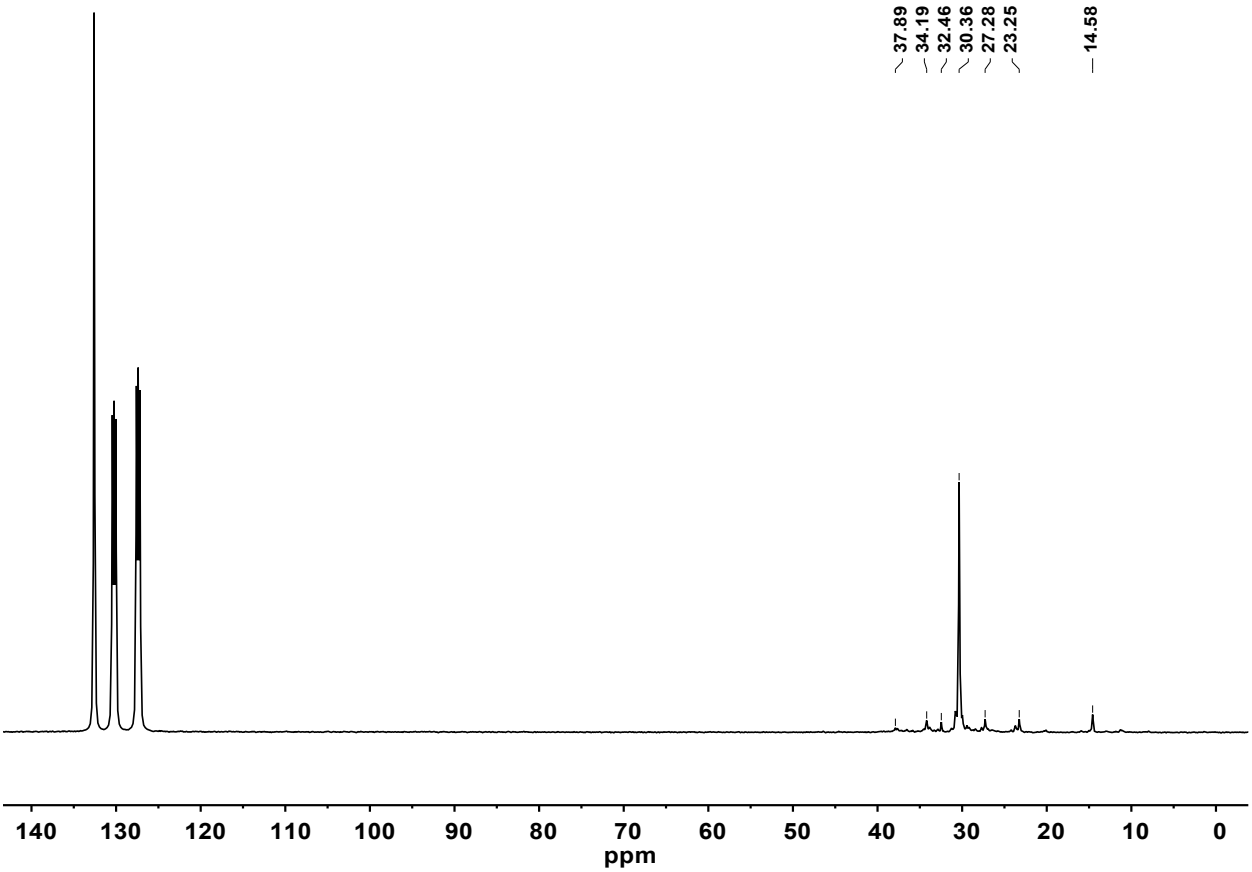

Figure S3. ^{13}C NMR spectrum (125 MHz, 25 °C, 1,2-dichlorobenzene-d4) of the high-quality liquid product (M_n = 1,200 Da) obtained with 5c-Pt/$SrTiO_3$ catalyst after 68 h.

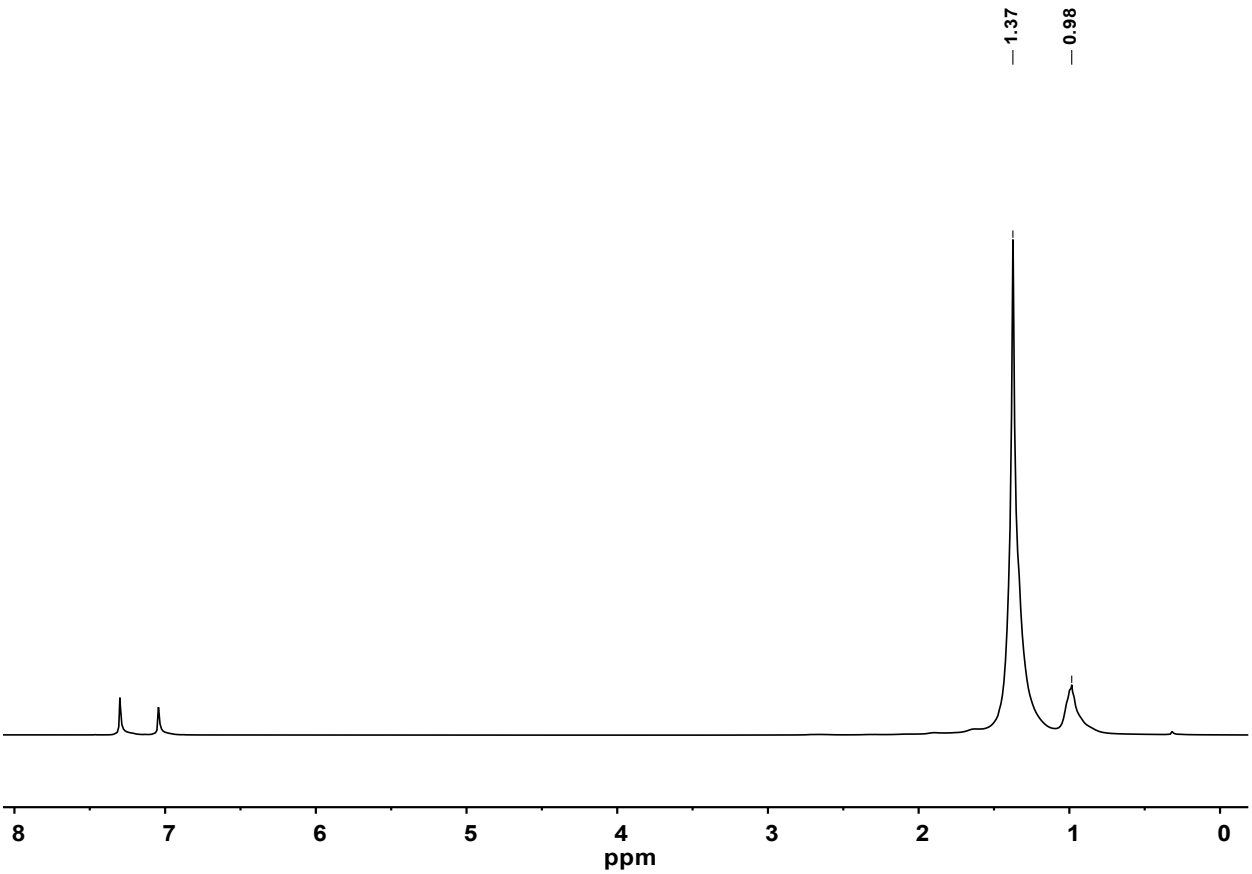

Figure S4. ^{1}H NMR spectrum (500 MHz, 25 °C, 1,2-dichlorobenzene) of the high-quality liquid product (M_n = 1200 Da) obtained with 5c-Pt/$SrTiO_3$ catalyst after 68 h. Long-chain branching was found to be 10 (see S1-C-iv).

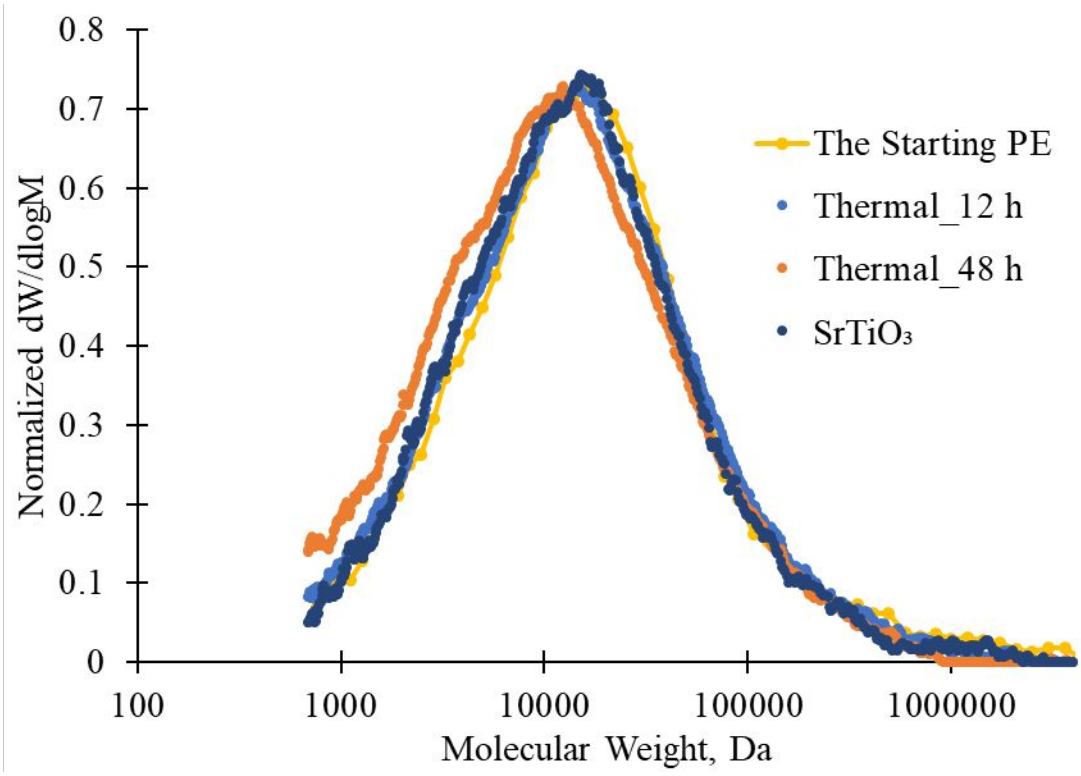

Figure S5. Comparison of GPC chromatographs of the starting PE (yellow), catalyst-free thermal reactions hydrogenolysis runs at 12 (blue) and 48 h (orange), and Pt-free $SrTiO_3$ (blue) for 24 h. Reaction conditions: 170 psi H_2, 300 °C, 50 mg PE (M_n = 8,150 Da), no catalyst or 10 mg $SrTiO_3$

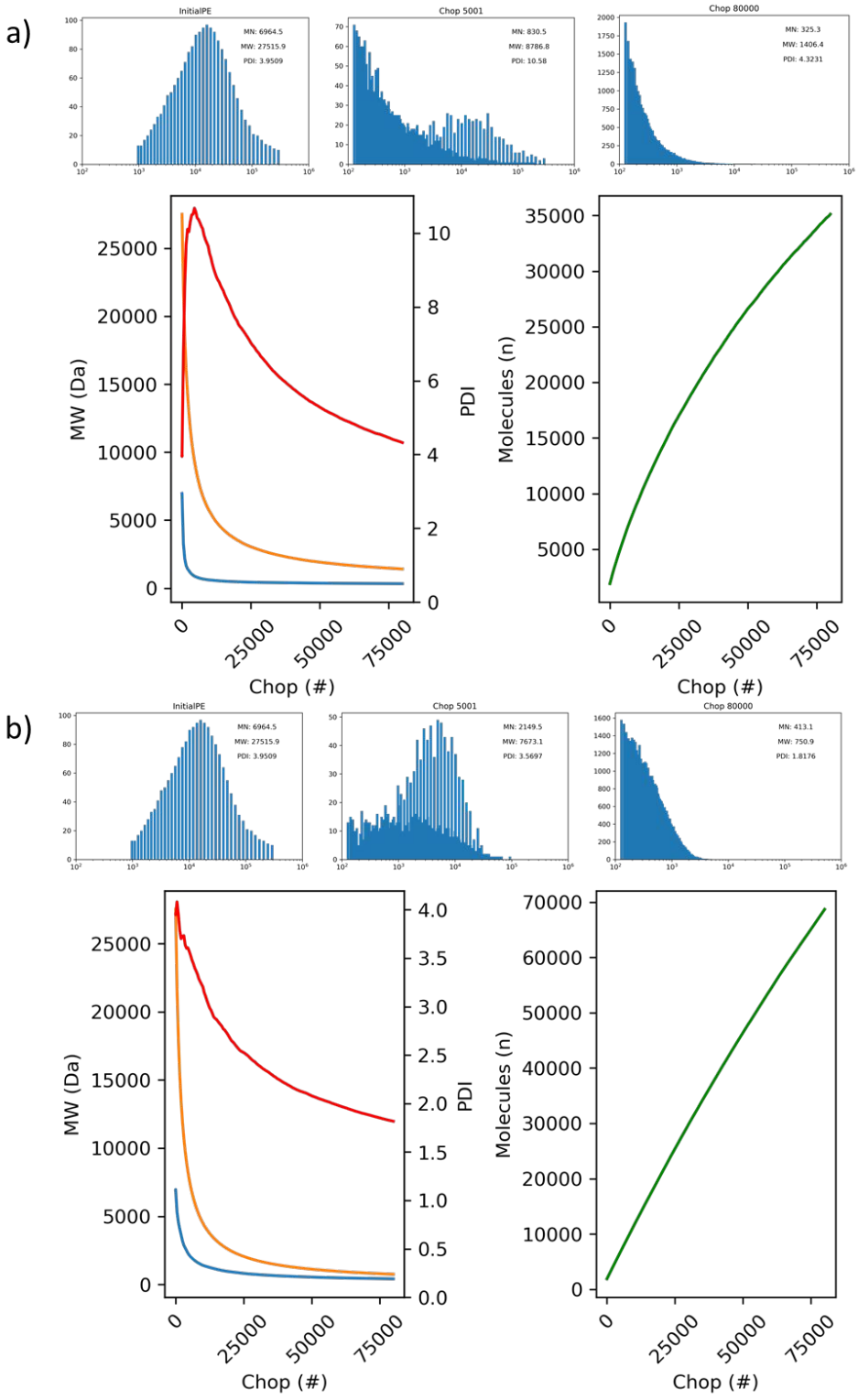

Figure S6. Numerical cleaving models of catalytic hydrogenolysis of polyethylene. The "random" model (a) assumes that all molecules have an equal probability of undergoing hydrogenolysis, while the "weighted" model (b) assumes that the hydrogenolysis is affected by adsorption of polyethylene to the catalyst and the probability is scaled linearly with the molecular weight. For

both models, the population is shown at three time points, initial, chop # 5,001, and chop # 80,000. The change in population with each hydrogenolytic chop is shown as M_n (blue), M_w (orange), Đ (red), and # of molecules greater than eight carbons (green). In the "random" model (a), the dispersity rapidly increases as the population spreads out, with many light molecules forming while most of the heavy molecules in initial sample still remain untouched. After reaching a maximum, dispersity starts to decrease as all molecules are randomly chopped. The number of molecules increases non-linearly, as many of the products are lost to the gas phase. In the "weighted" model (b), as the polyethylene is chopped by the catalyst, the population shifts to lower molecular weights, and the distribution narrows. The narrowing of the distribution can be seen in the dispersity, which initially decreases rapidly, and then plateaus. The behavior of the "weighted" model (b) more closely matches the change with time of the $Pt/SrTiO_3$ catalysts, and suggests that 1) the adsorption of the polyethylene to the catalyst has a significant effect on the product distribution and 2) that the slowing of the change in Đ is an effect of the increase in the number of alkane molecules with time rather than a deactivation of the catalyst.

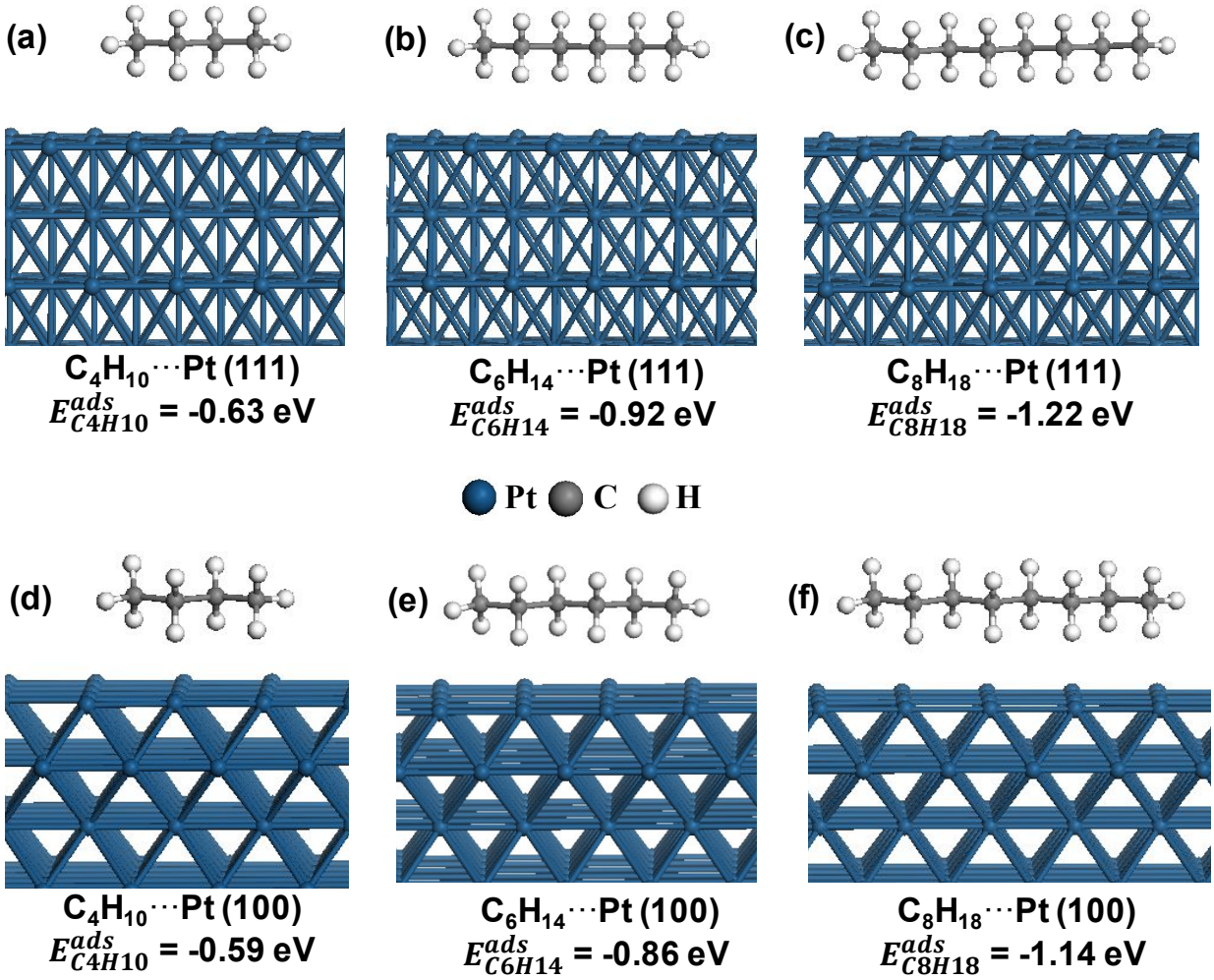

Figure S7. Side view of the optimized structures of (a) *n*-butane, (b) *n*-hexane, and (c) *n*-octane on Pt (111) surface model and (d) *n*-butane, (e) *n*-hexane, and (f) *n*-octane on Pt (100) surface model.

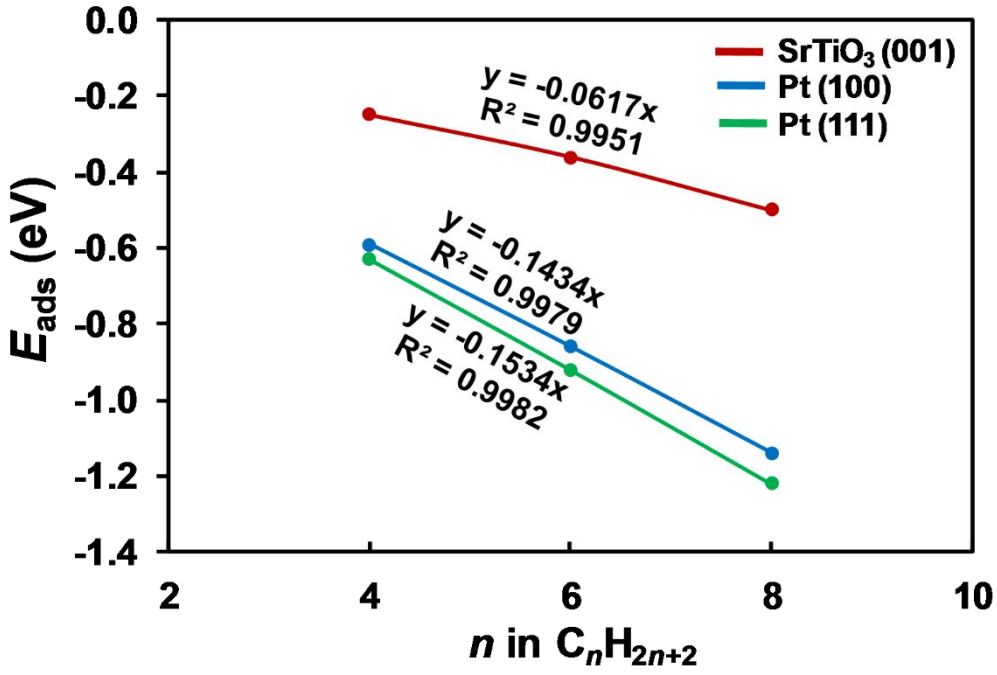

Figure S8. Adsorption energies (E_{ads}) of *n*-alkanes on Pt and $SrTiO_3$ surface models.

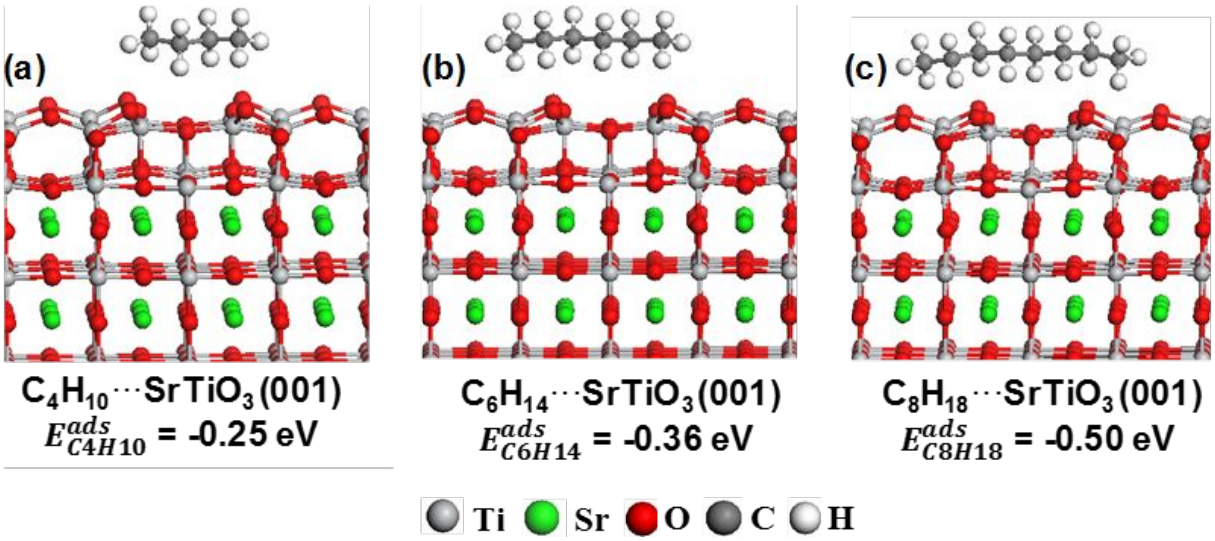

Figure S9. Side view of the optimized structures of (a) *n*-butane, (b) *n*-hexane, and (c) *n*-octane on TiO_2 double-layer terminated $SrTiO_3$ (001) surface model.

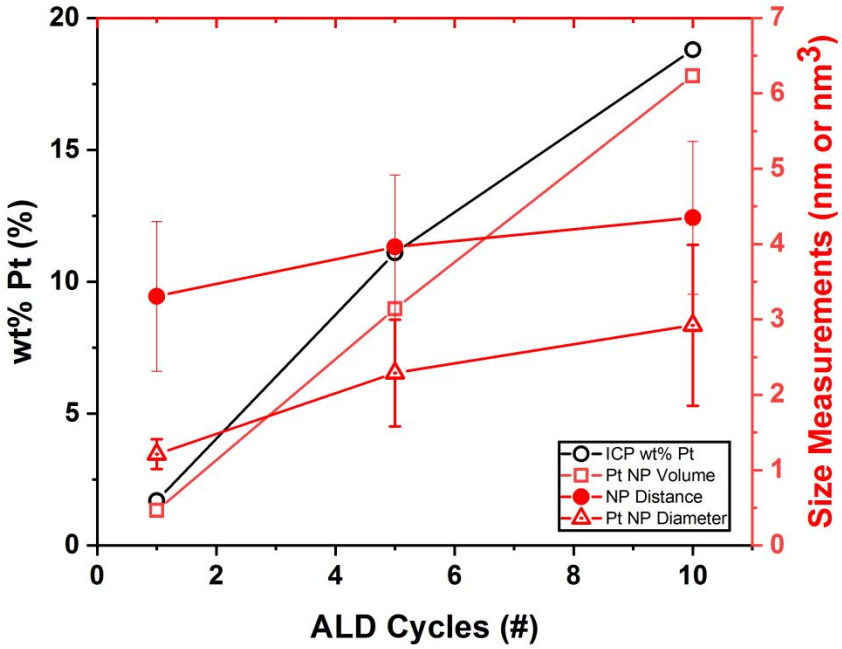

Figure S10. Plot of properties of the catalysts with varying number of Pt ALD cycles (1, 5, and 10) and corresponding Pt wt% (determined by ICP), Pt NP diameter (measured by TEM), Pt NP distances (measured by TEM), and Pt NP volume (calculated from Pt NP diameters). A linear regression shows a growth rate of 1.9 ± 0.2 wt % Pt per ALD cycle.

Table S2. Properties of 1c,5c, and 10c-Pt/$SrTiO_3$.

Catalysts	Pt loading[a] wt%	Average Pt size[b] nm	Average Pt edge (nm) to face (nm^2) ratio[c]	Average Pt surface area (m^2 Pt/g cat.)[d]	Average Pt NP center-center dist.[b] nm
1c-Pt/$SrTiO_3$	1.7	1.2	0.265	5.9	3.3
5c-Pt/$SrTiO_3$	11.1	2.3	0.138	20.0	4.0
10c-Pt/$SrTiO_3$	18.8	2.9	0.109	26.8	4.4

[a]Determined by ICP-OES. [b]Determined by TEM particle size analysis. [c]Pt NPs approximated as Winterbottom constructions, with $\gamma_{Pt\{111\}}:\gamma_{Pt\{100\}} = 0.84$, Pt(100)||$SrTiO_3$(100) at 61% truncation. [d]Surface area calculated from Pt loading and average particle size, assuming the minimum energy Winterbottom construction.

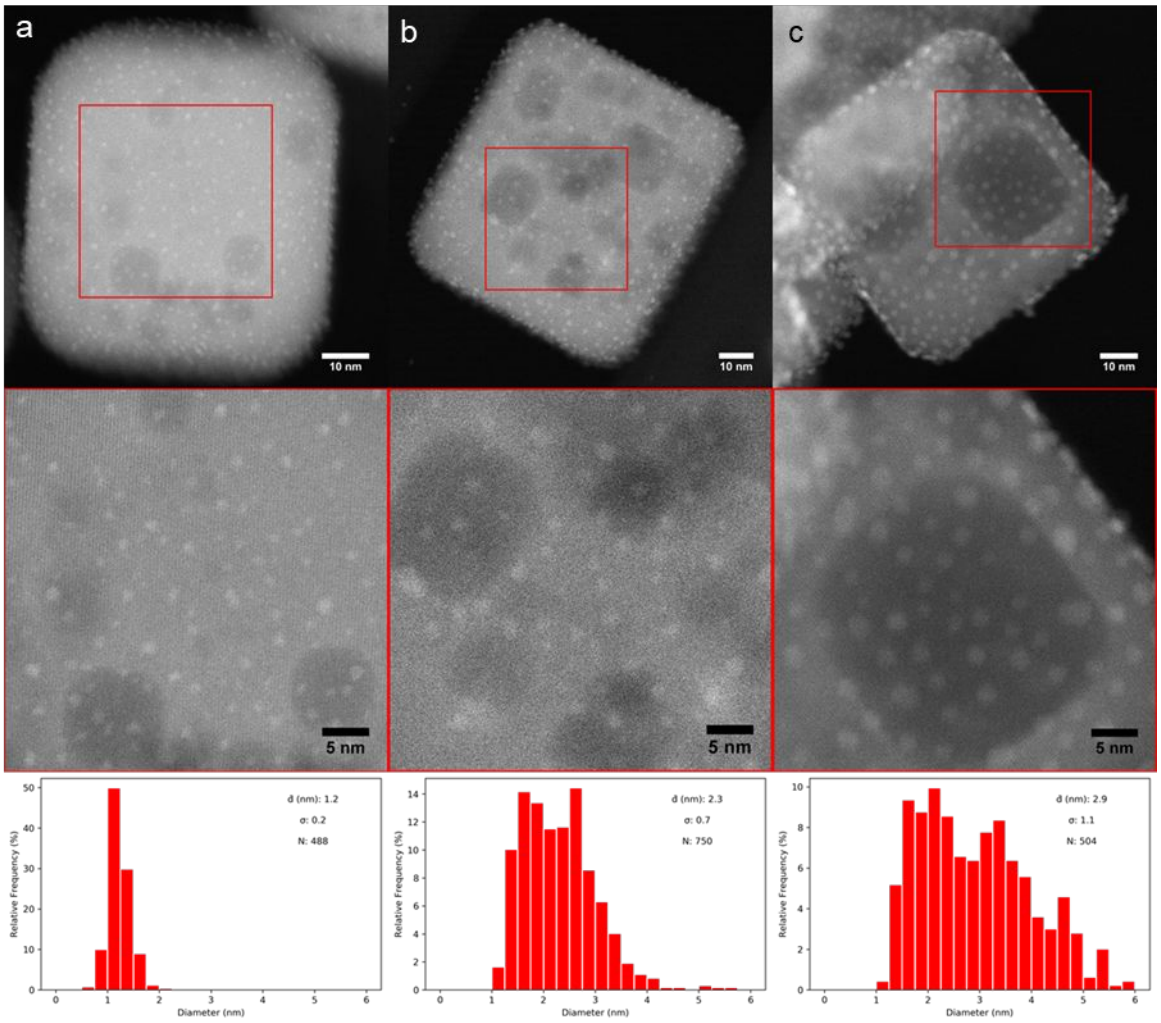

Figure S11. Electron micrographs of Pt nanoparticles with an average size of a) 1.2 ± 0.2 nm , b) 2.3 ± 0.7 nm, and c) 2.9 ± 1.1 nm, deposited by ALD on $SrTiO_3$ nanocuboid supports, via (respectively) 1, 5, and 10 ALD cycles. The region highlighted in red is shown as an enlarged inset.

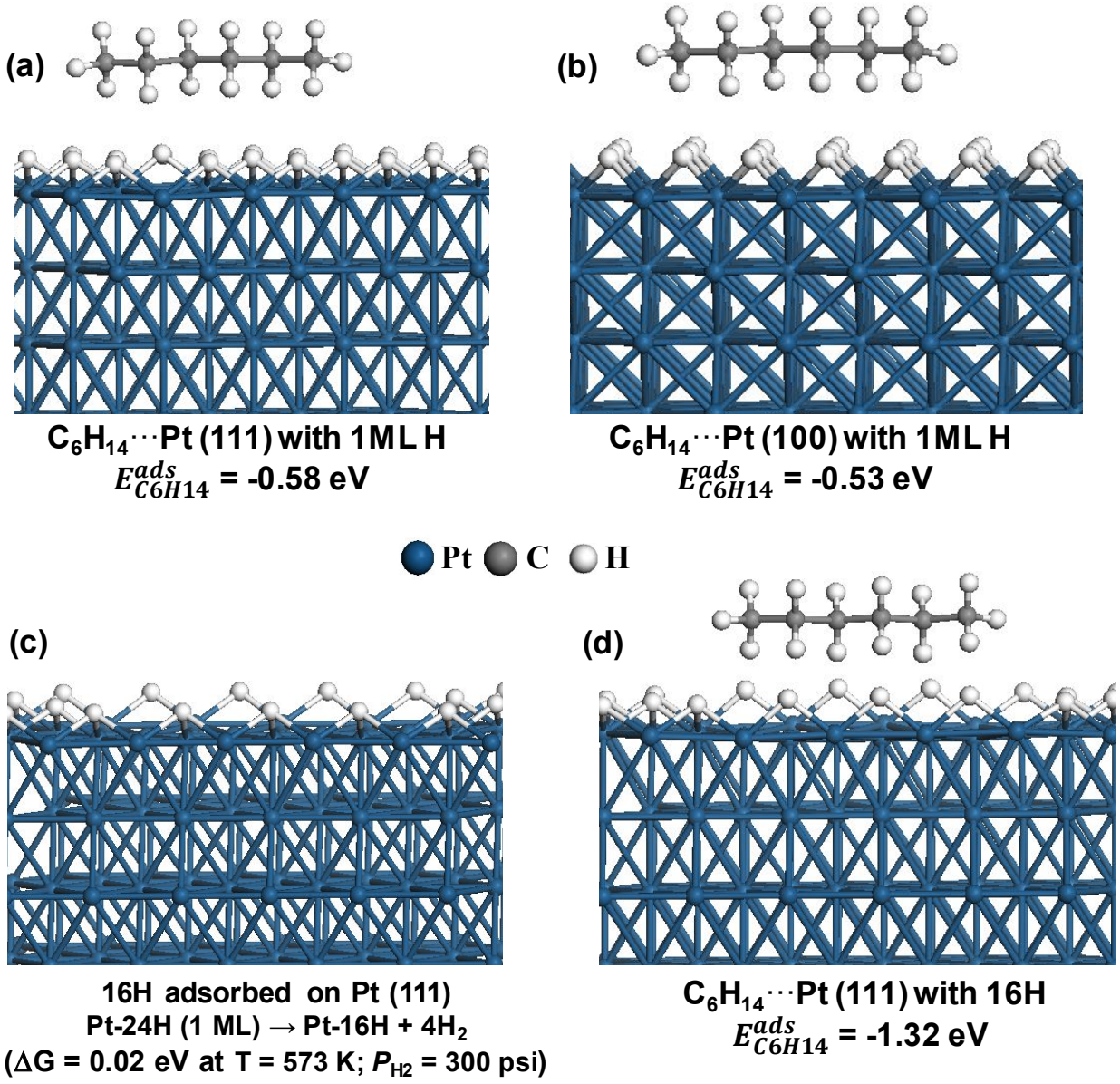

Figure S12. Side view of the optimized structures of hexane adsorbed on 1 ML hydrogen covered (a) Pt (111) and (b) Pt (100) surface models. Reaction free energy presented under structure (c) suggests that removing H atoms from Pt (111) surface is favorable under reaction conditions and the hexane adsorption becomes stronger in the presence of few H atoms as shown under structure (d). Under similar conditions, removing a single H atom from the 1 ML H-covered Pt (100) surface was found to be endergonic by 0.51 eV. It has been assumed here that the free energy of adsorption of a large hydrocarbon chain is approximately equal to its adsorption energy considering that the entropy contribution per carbon atoms becomes negligible for increasingly large polymer chains.

Table S3. Properties of the starting PE, hydrogenolyzed products and number of light hydrocarbons formed over thermal hydrogenolysis, 5c-Pt/$SrTiO_3$, and Pt/Al_2O_3 using the Parr reactor. Reaction conditions: 170 psi H_2, 300 °C, 18 h, and 3 g PE, and 8 mg of Pt as 5c-Pt/$SrTiO_3$.

Entry	M_n, Da	M_w, Da	$Đ$	Light HCs (C_1-C_8) formed, mmol
PE	8,150	22,150	2.7	n/a
Thermal Hydrogenolysis	4,550	18,600	4.1	0.65
5c-Pt/$SrTiO_3$	2,050	5,800	2.8	1.17
Pt/Al_2O_3	1,850	10,750	5.8	2.34

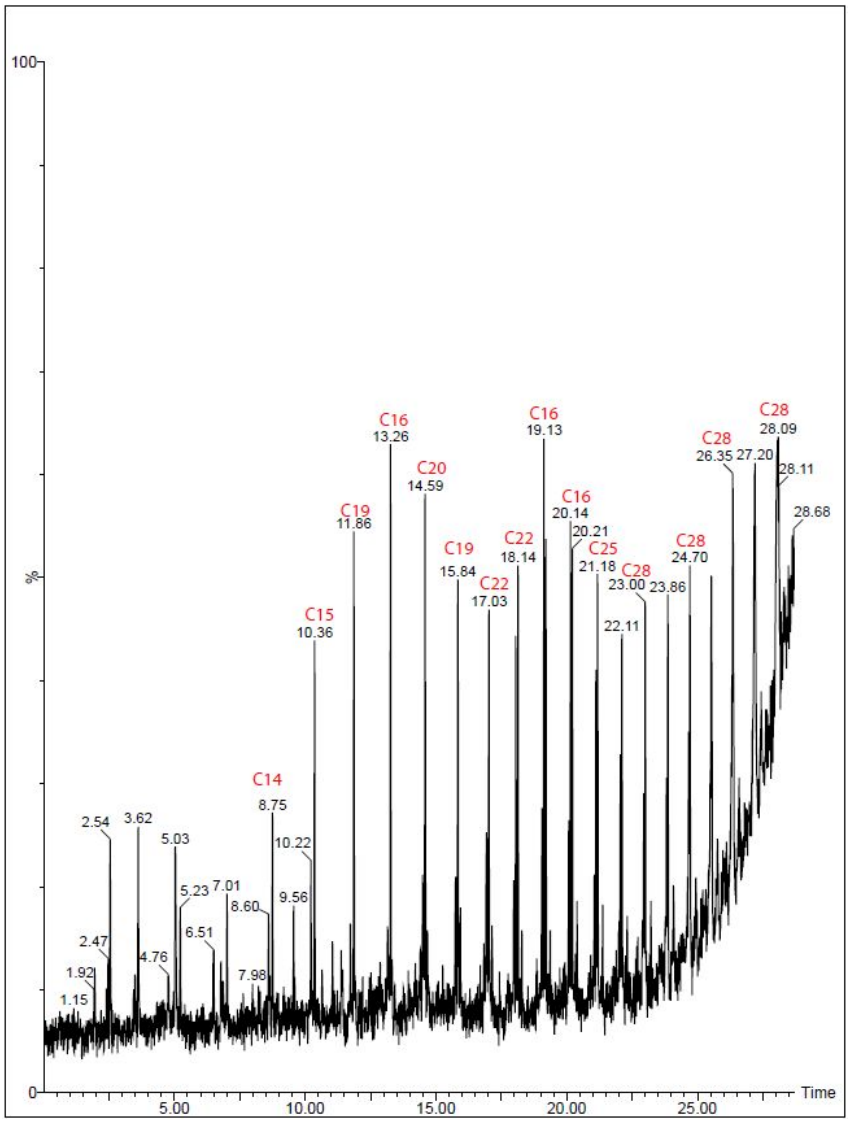

Figure S13. Pyrolysis GC-MS chromatograms of hydrogenolyzed product obtained over Pt/Al_2O_3.

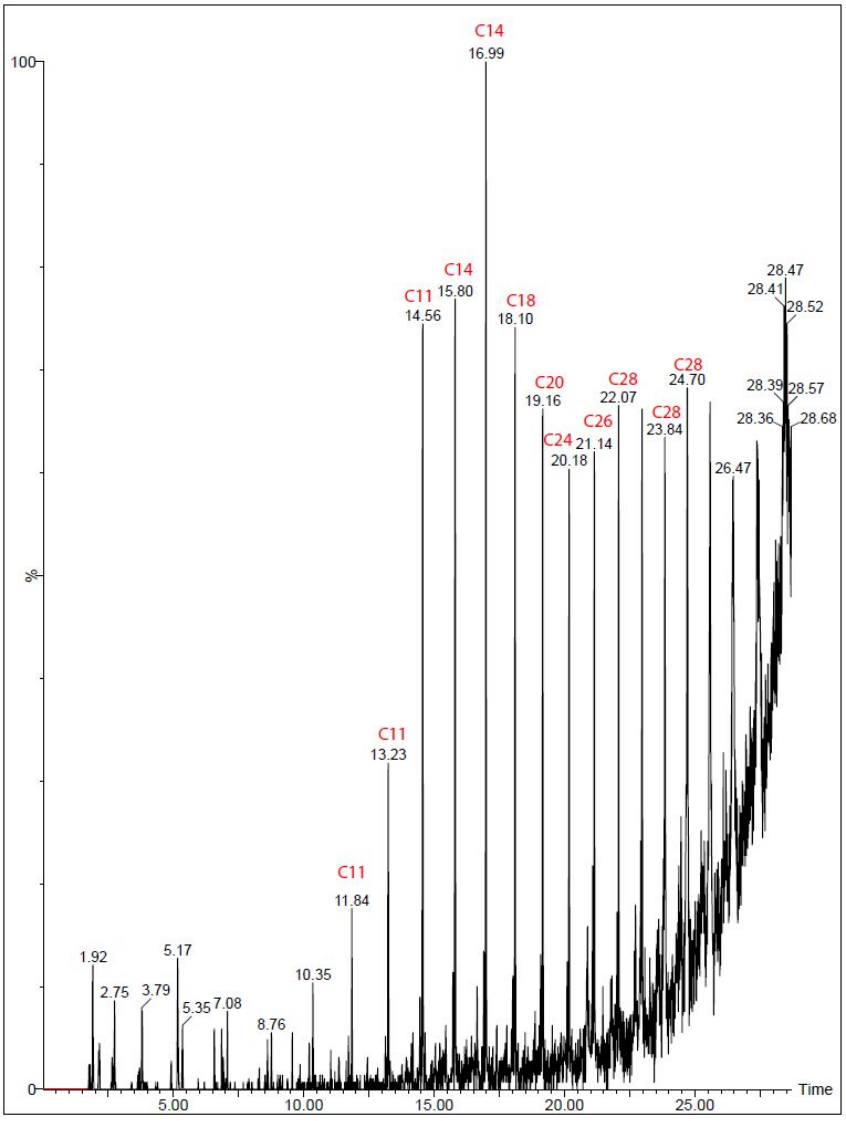

Figure S14. Pyrolysis GC-MS chromatograms of hydrogenolyzed product obtained over 5c-Pt/$SrTiO_3$.

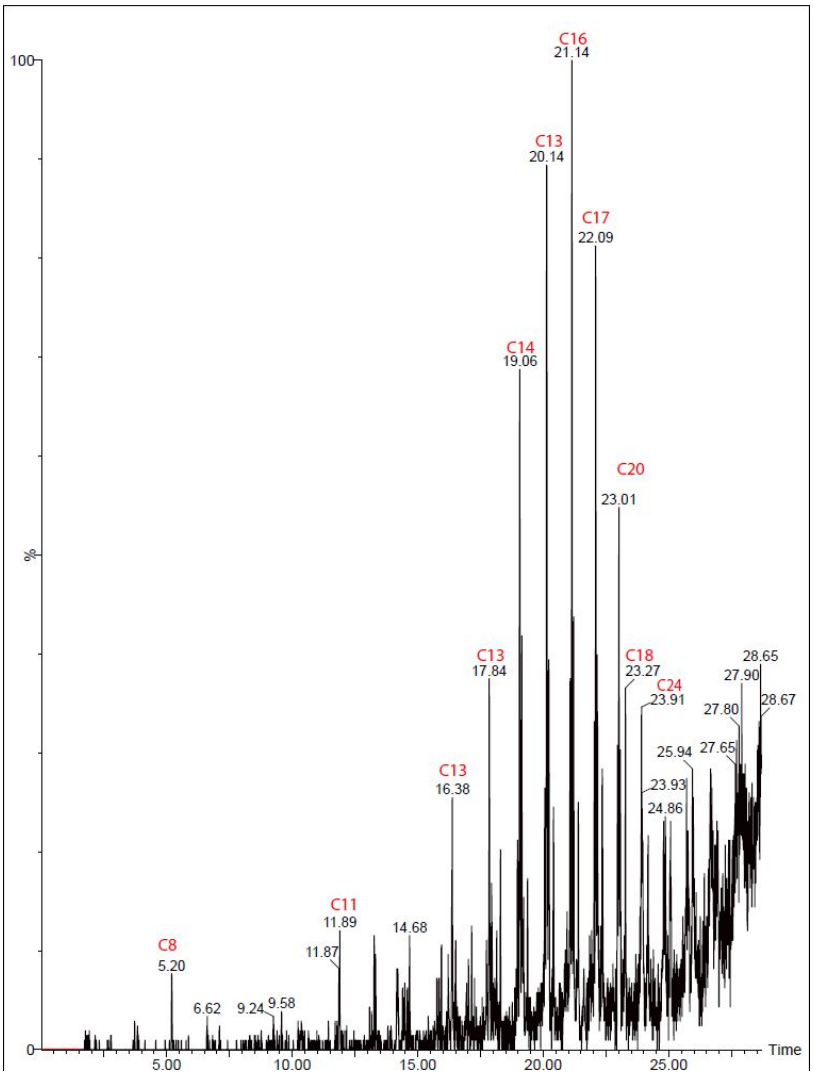

Figure S15. Pyrolysis GC-MS chromatograms of hydrogenolyzed product obtained over thermal hydrogenolysis.

Figures S13-S15 depict chromatograms of species thermally desorbed from hydrogenolyzed product mixture obtained over Pt/Al_2O_3, $Pt/SrTiO_3$, and from thermal hydrogenolysis, respectively. Peaks of chromatograms were matched to a carbon number using NIST mass spectral database using MassLynx software. TD chromatograms of product mixtures of Pt/Al_2O_3 (Figure S13) and $Pt/SrTiO_3$ (Figure S14) have significant overlap for similar carbon numbered species while product mixture obtained from $Pt/SrTiO_3$ are composed of higher carbon number species. Both product mixtures contain significant amount of C_{28} species. In contrast, the TD chromatogram of products obtained through thermal hydrogenolysis (Figure S15) reveal species containing lower carbon numbers in comparison with Pt/Al_2O_3, $Pt/SrTiO_3$. Biggest peak observed for thermal hydrogenolysis was determined to be a C_{16} species. Together, these data suggest that $Pt/SrTiO_3$ catalytic hydrogenolysis is selective for products with a cutoff minimum molecular weight.

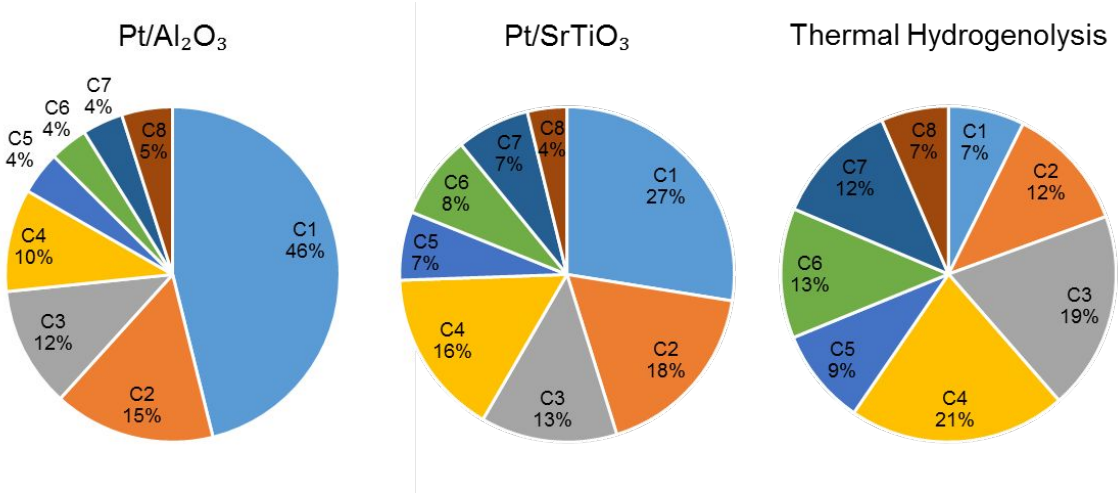

Figure S16. C_1-C_8 light hydrocarbon distribution of head-space analysis over Pt/Al_2O_3, 5c-$Pt/SrTiO_3$, and thermal hydrogenolysis. Reaction Conditions: 170 psi H_2, 300 °C, 18 h, 3 g PE, and no catalyst (thermal hydrogenolysis) or 8 mg Pt as 5c-$Pt/SrTiO_3$ or Pt/Al_2O_3.

Table S4. Properties of 5c-Pt/$SrTiO_3$ and Pt/Al_2O_3 used in batch reactor experiments, initial and after 18 h in batch reactor.

Catalysts	Pt loading[a] wt%	Average Pt size[b] nm	Average Pt edge (nm) to face (nm^2) ratio[c]	Average Pt surface area (m^2 Pt/g cat.)[d]
5c-Pt/$SrTiO_3$	7.3	2.0 ± 0.5	0.159	15.1
5c-Pt/$SrTiO_3$ 18 h	7.3	2.1 ± 0.5	0.151	14.4
Pt/Al_2O_3	0.7	1.2 ± 0.4	0.306	1.7
Pt/Al_2O_3 18 h	0.7	1.6 ± 0.4	0.228	1.3

[a]Determined by ICP-OES. [b]Determined by TEM particle size analysis. [c]Pt NPs approximated as Winterbottom constructions, with $\gamma_{Pt\{111\}}:\gamma_{Pt\{100\}} = 0.84$, Pt(100)||$SrTiO_3$(100) at 61% truncation, and Pt(100)||γ-Al_2O_3(111) at 16% truncation. [d]Surface area calculated from Pt loading and average particle size, assuming the minimum energy Winterbottom construction.

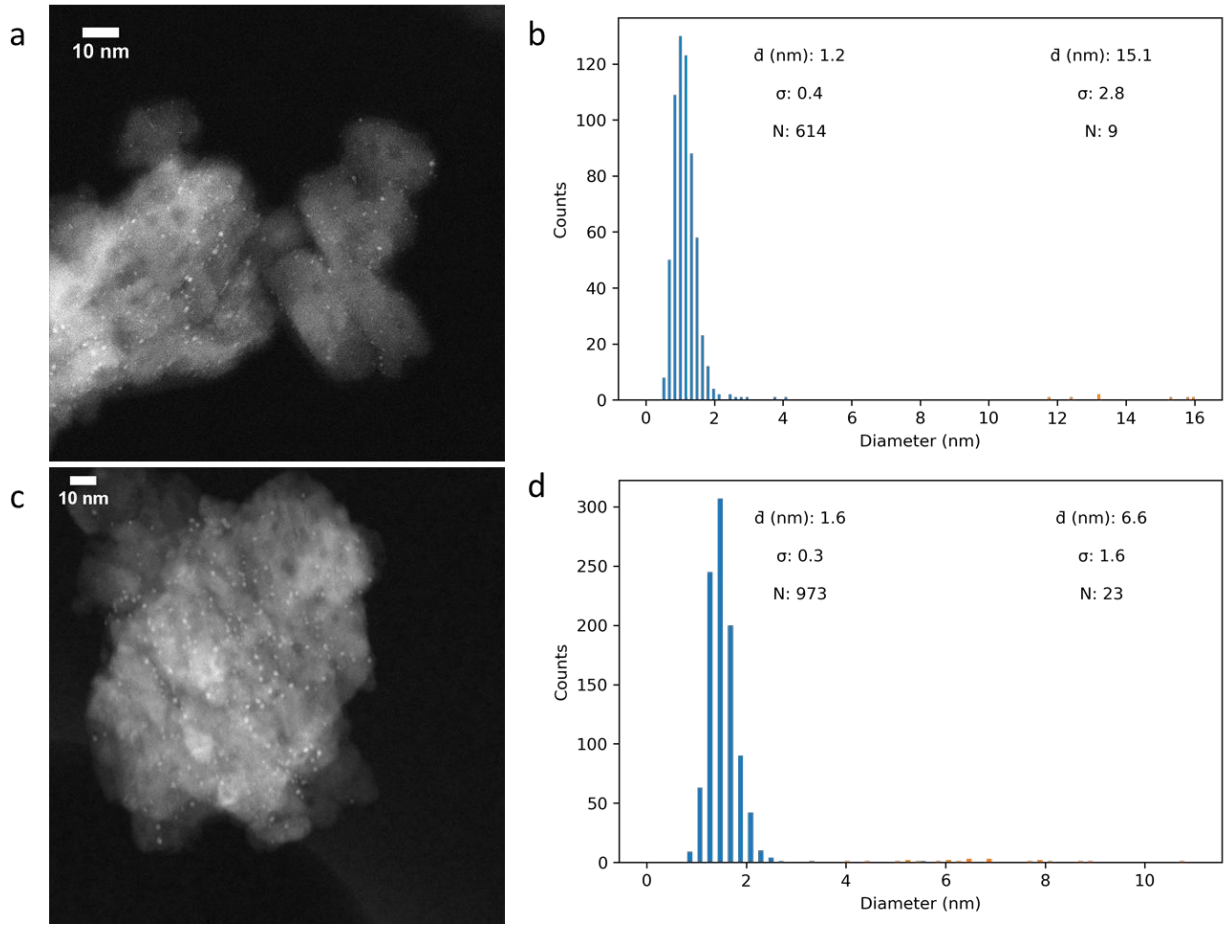

Figure S17. Electron micrograph(s) of Pt/Al_2O_3 with a histogram showing the particle size distribution (a,b) as synthesized, (c,d) after 18 hours of PE hydrogenolysis in a batch reactor. The Pt NP distribution can be described as bimodal, with sub-2nm particles and >5nm particles.

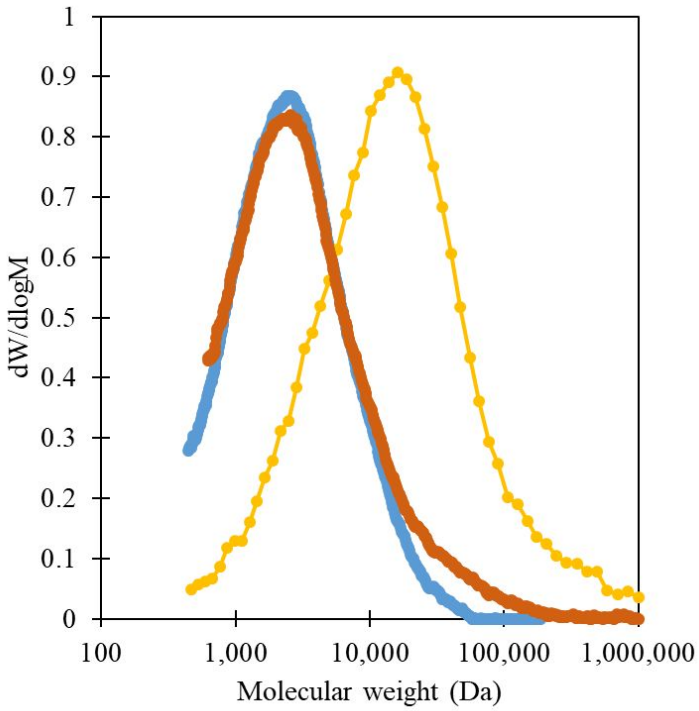

Figure. S18 Comparison of GPC chromatographs of 1c-Pt/$SrTiO_3$ (blue) and 1wt% Pt/Al_2O_3 (Aldrich, orange) at equal area time (surface area of Pt multiplied by reaction time) at 300 °C and 170 psi. 1c-Pt/$SrTiO_3$ (12 hours, 10 mg, 0.71 m^2 Pt x h) has a M_n of 1,550 Da and $Đ$ of 2.4, while Pt/Al_2O_3 (48 hr, 10 mg, 0.83 m^2 Pt x h) has a M_n of 1,450 Da and $Đ$ of 6.6.

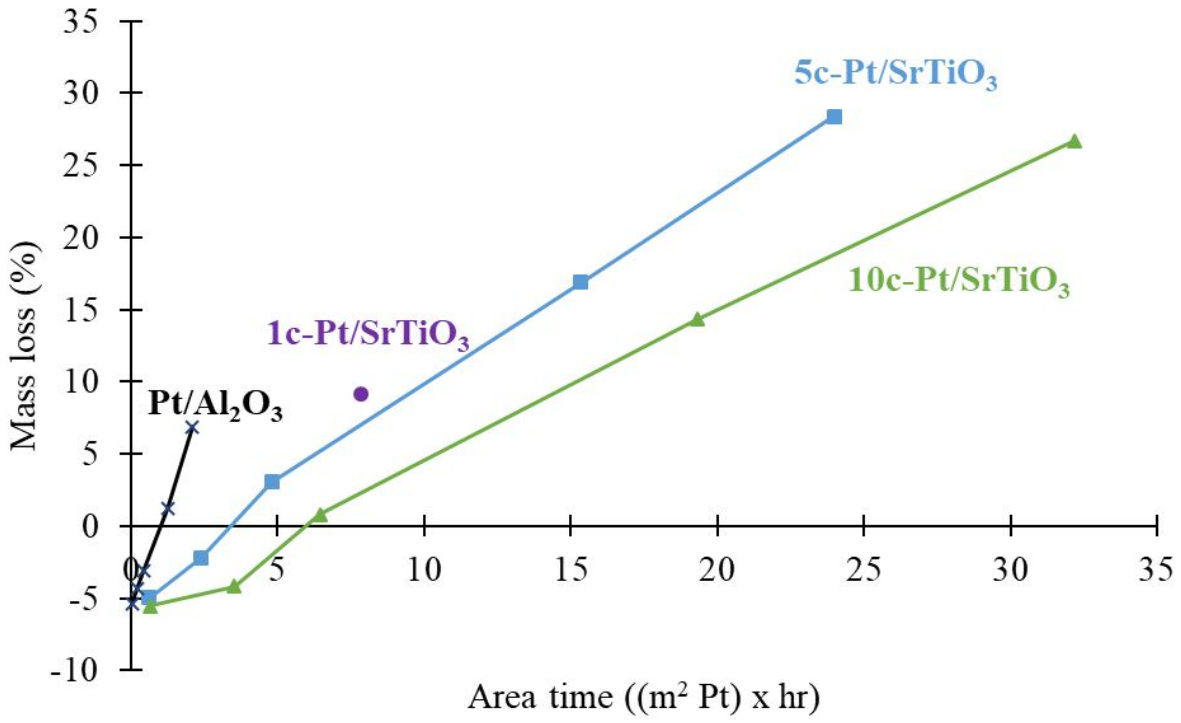

Figure S19. Mass loss versus area time (surface area of Pt multiplied by reaction time) for 1wt% Pt/Al_2O_3 (black X, 1.2 nm Pt), 1c-$Pt/SrTiO_3$ (purple circle, single point, 1.2 nm Pt), 5c-$Pt/SrTiO_3$ (light blue square, 2.3 nm Pt), and 10c-$Pt/SrTiO_3$ (green triangle, 2.9 nm Pt). The rate of change increases as the Pt particle size on $SrTiO_3$ decreases, corresponding to an increase in edge sites. Reaction Conditions: 300 °C, 170 psi, 24 h. SPR.

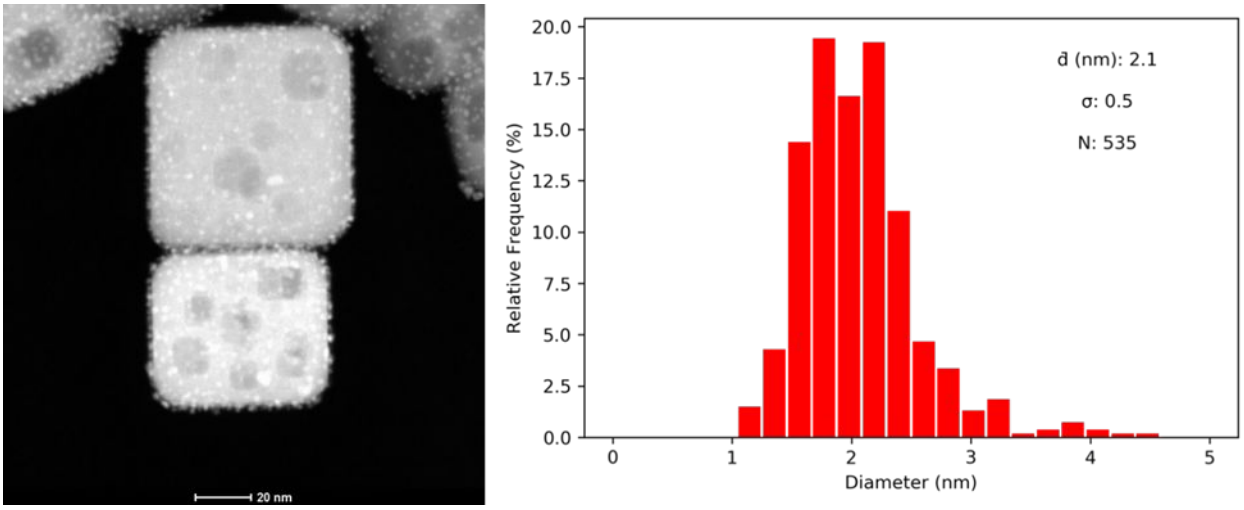

Figure S20. Electron micrograph and histogram of 5c-Pt/$SrTiO_3$ after 18 h of PE hydrogenolysis in a batch reactor.

TEM images of Pt NPs on γ-Al_2O_3 (Figure S17) reveal that the average particle size is 1.2 ± 0.4 nm and after 18 h of PE hydrogenolysis is 1.6 ± 0.4 nm. The average Pt particle diameter for 5c-Pt/$SrTiO_3$ increased from 2.0 ± 0.5 nm to 2.1 ± 0.5 nm after 18 h (Figure 1 and Figure S20). The negligible change in particle size of Pt in 5c-Pt/$SrTiO_3$ suggests that the stabilization of Pt by $SrTiO_3$ relative to γ-Al_2O_3 is effective in minimizing the effect of sintering under reaction conditions. Note that, platinum has a weaker interfacial interaction with γ-Al_2O_3 than with $SrTiO_3$ and the minimum energy Winterbottom shape of Pt on γ-Al_2O_3 is closer to that of a free Wulff particle, facilitating the sintering.

Table S5. Properties of the hydrogenolyzed products over pristine and post-reaction 5c-Pt/$SrTiO_3$ using the SPR. Reaction conditions: 170 psi H_2, 300 °C, 24 h, 50 mg PE (M_n = 8,150 Da), 0.7 mg of Pt as 5c-Pt/$SrTiO_3$ (7.3 wt% Pt).

Entry	M_n, Da	$Đ$
5c-Pt/$SrTiO_3$ - Pristine	1,100	1.7
5c-Pt/$SrTiO_3$ - Post-Reaction	2,800	2.2

S3. Determination of PE branching

Table S6. Properties of PE substrates

PE Substrates	Supplier	Product Number	M_n,[a] Da	M_w,[a] Da	$Đ^+$	Branches/1000C[b]
PE	Sigma-Aldrich	427799	8,150	22,150	2.7	2
PE	Scientific Polymer Products, Inc.	562	15,400	17,200	1.1	10[c]
PE	Scientific Polymer Products, Inc.	1018	64,300	70,400	1.1	20[c]
PE	Scientific Polymer Products, Inc.	565	158,000	420,000	2.7	20[c]
Plastic Bag	Aspen - Can Liners, North American Corporation	380414	33,000	115,150	3.5	2

[a]Determined by GPC. [b]Determined by ^{1}H NMR using the following formula: branches per 1000 carbons = $(CH_3/3)/\{(CH + CH_2 + CH_3)/2\}$ x 1000. CH_3, CH_2, and CH refer to the integrations obtained for the methyl, methylene, and methine resonances, respectively. The NMR spectra for PE (Sigma-Aldrich, 427799) and plastic bag (Aspen – Can Liners, North American Corporation 380414) are shown in Figure S21 and S22, respectively.[S12,S13] [c]Obtained from the PE substrate certificates shown in Figure S23-S25.

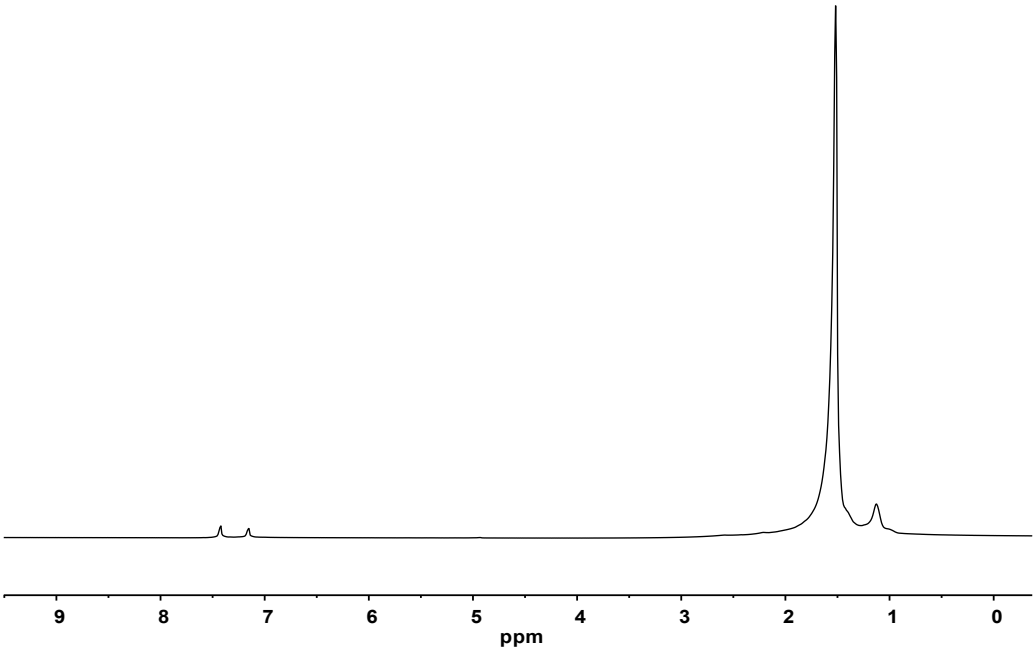

Figure S21. ^{1}H NMR spectrum (500 MHz, 80 °C, 1,2-dichlorobenzene) of the PE substrate (Sigma-Aldrich, Product number = 427799).

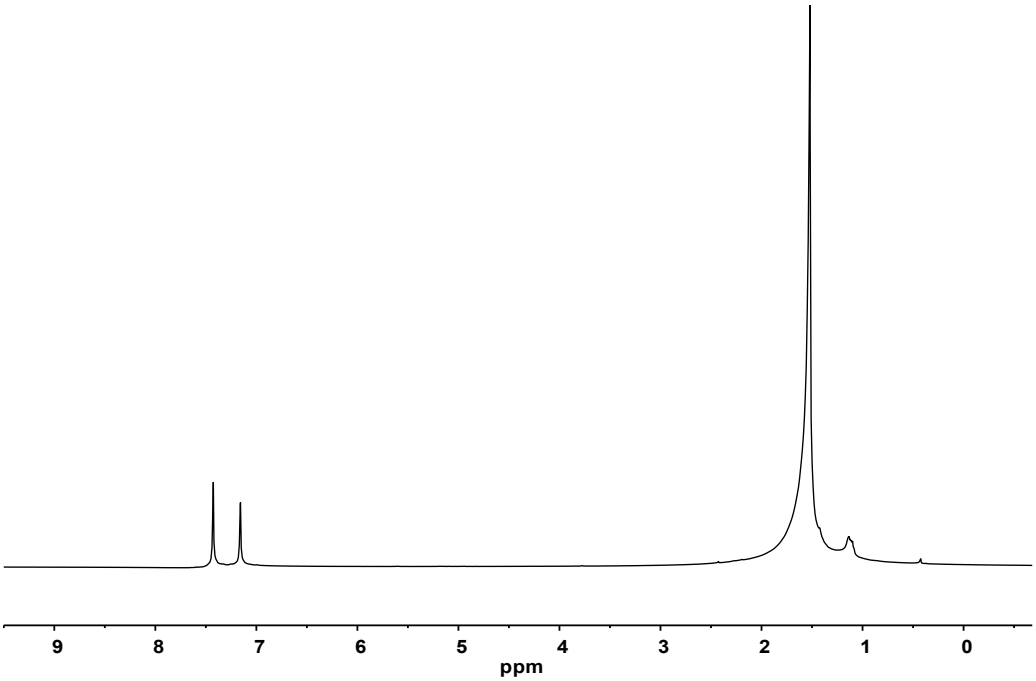

Figure S22. ^{1}H NMR spectrum (500 MHz, 80 °C, 1,2-dichlorobenzene) of the plastic bag (Aspen Can Liners, North American Corporation, Product number = 380414).

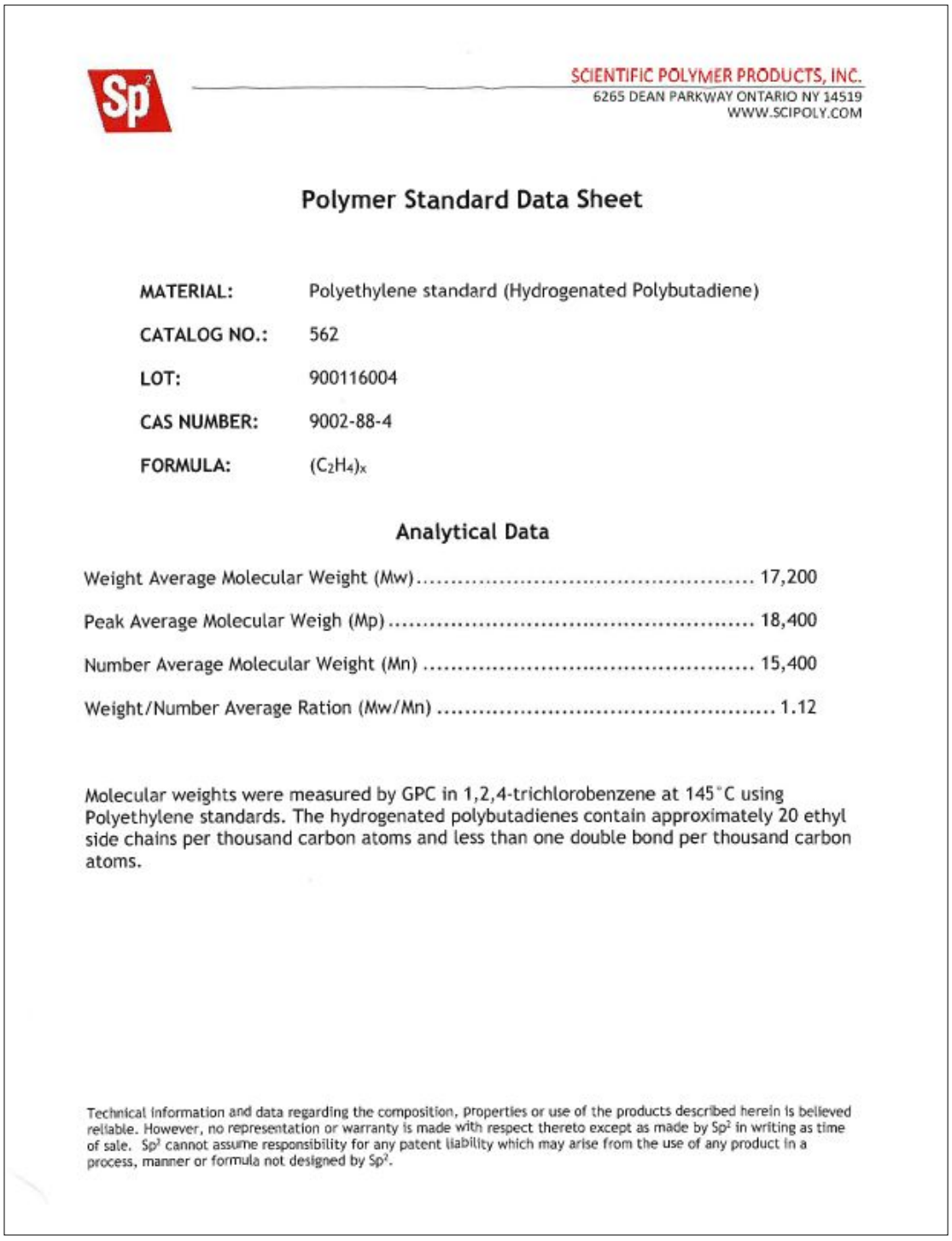

SCIENTIFIC POLYMER PRODUCTS, INC.
6265 DEAN PARKWAY ONTARIO NY 14519
WWW.SCIPOLY.COM

Polymer Standard Data Sheet

MATERIAL:	Polyethylene standard (Hydrogenated Polybutadiene)
CATALOG NO.:	562
LOT:	900116004
CAS NUMBER:	9002-88-4
FORMULA:	$(C_2H_4)_x$

Analytical Data

Weight Average Molecular Weight (Mw)..... 17,200

Peak Average Molecular Weigh (Mp)..... 18,400

Number Average Molecular Weight (Mn)..... 15,400

Weight/Number Average Ration (Mw/Mn)..... 1.12

Molecular weights were measured by GPC in 1,2,4-trichlorobenzene at 145°C using Polyethylene standards. The hydrogenated polybutadienes contain approximately 20 ethyl side chains per thousand carbon atoms and less than one double bond per thousand carbon atoms.

Technical information and data regarding the composition, properties or use of the products described herein is believed reliable. However, no representation or warranty is made with respect thereto except as made by Sp² in writing as time of sale. Sp² cannot assume responsibility for any patent liability which may arise from the use of any product in a process, manner or formula not designed by Sp².

Figure S23. Polymer Standard Data Sheet for PE substrate (Scientific Polymer, Product number = 562).

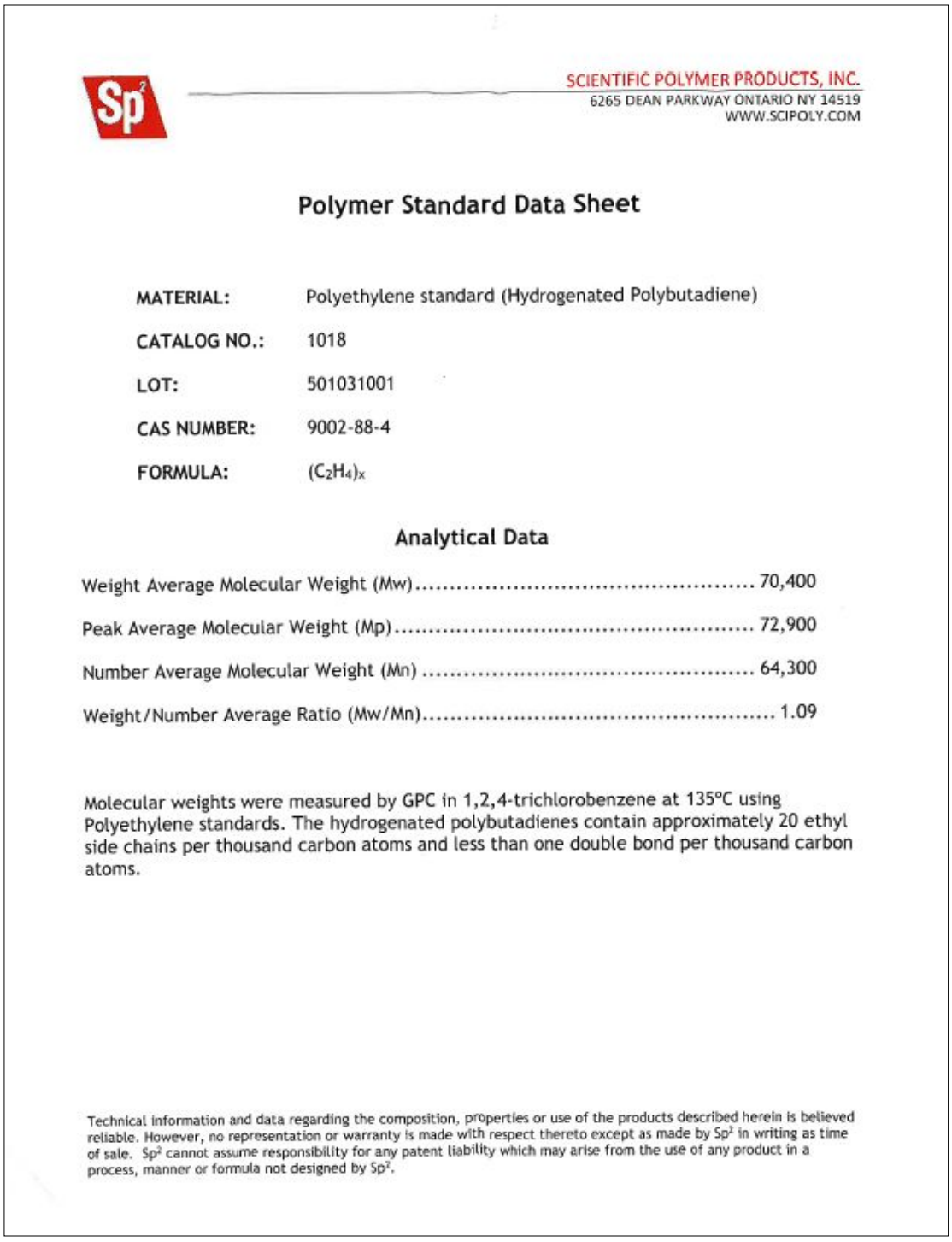

SCIENTIFIC POLYMER PRODUCTS, INC.
6265 DEAN PARKWAY ONTARIO NY 14519
WWW.SCIPOLY.COM

Polymer Standard Data Sheet

MATERIAL:	Polyethylene standard (Hydrogenated Polybutadiene)
CATALOG NO.:	1018
LOT:	501031001
CAS NUMBER:	9002-88-4
FORMULA:	$(C_2H_4)_x$

Analytical Data

Weight Average Molecular Weight (Mw)	70,400
Peak Average Molecular Weight (Mp)	72,900
Number Average Molecular Weight (Mn)	64,300
Weight/Number Average Ratio (Mw/Mn)	1.09

Molecular weights were measured by GPC in 1,2,4-trichlorobenzene at 135°C using Polyethylene standards. The hydrogenated polybutadienes contain approximately 20 ethyl side chains per thousand carbon atoms and less than one double bond per thousand carbon atoms.

Technical information and data regarding the composition, properties or use of the products described herein is believed reliable. However, no representation or warranty is made with respect thereto except as made by Sp² in writing as time of sale. Sp² cannot assume responsibility for any patent liability which may arise from the use of any product in a process, manner or formula not designed by Sp².

Figure S24. Polymer Standard Data Sheet for PE substrate (Scientific Polymer, Product number = 1018).

SCIENTIFIC POLYMER PRODUCTS, INC.
6265 DEAN PARKWAY ONTARIO NY 14519
WWW.SCIPOLY.COM

Polymer Standard Data Sheet

MATERIAL: Polyethylene standard (Hydrogenated Polybutadiene)

CATALOG NO.: 565

LOT: 980702001

CAS NUMBER: 9002-88-4

FORMULA: $(C_2H_4)_x$

Analytical Data

Weight Average Molecular Weight (Mw) 420,000

Number Average Molecular Weight (Mn)..... 158,000

Weight/Number Average Ratio (Mw/Mn) 2.66

All samples contain approximately 0.05 percent Ionol antioxidant.
The hydrogenated polybutadienes contain approximately 20 ethyl side chains per thousand carbon atoms and less than one double bond per thousand carbon atoms.

The weight average molecular weights were determined by scattered light photometry in alpha-chloronaphthalene at 140°C. Corrections were made to the intensities for any observed anisotropy. Number average molecular weights were determined by membrane osmometry in alpha-chloronaphthalene at 130°C.

Technical information and data regarding the composition, properties or use of the products described herein is believed reliable. However, no representation or warranty is made with respect thereto except as made by Sp² in writing as time of sale. Sp² cannot assume responsibility for any patent liability which may arise from the use of any product in a process, manner or formula not designed by Sp².

Figure S25. Polymer Standard Data Sheet for PE substrate (Scientific Polymer, Product number = 565).

S4. References

(S1) Rabuffetti, F. A.; Kim, H.-S.; Enterkin, J. A.; Wang, Y.; Lanier, C. H.; Marks, L. D.; Poeppelmeier, K. R.; Stair, P. C. Synthesis-dependent first-order Raman scattering in $SrTiO_3$ nanocubes at room temperature. *Chem. Mater.* **2008,** *20* (17), 5628-5635.

(S2) Christensen, S. T.; Elam, J. W.; Rabuffetti, F. A.; Ma, Q.; Weigand, S. J.; Lee, B.; Seifert, S.; Stair, P. C.; Poeppelmeier, K. R.; Hersam, M. C.et al. Controlled growth of platinum nanoparticles on strontium titanate nanocubes by atomic layer deposition. *Small* **2009,** *5* (6), 750-757.

(S3) Staykov, A.; Fukumori, S.; Yoshizawa, K.; Sato, K.; Ishihara, T.; Kilner, J. Interaction of SrO-terminated $SrTiO_3$ surface with oxygen, carbon dioxide, and water. *J. Mater. Chem. A* **2018,** *6* (45), 22662-22672.

(S4) Lee, H.-B.-R.; Pickrahn, K. L.; Bent, S. F. Effect of O_3 on growth of Pt by atomic layer deposition. *J. Phys. Chem. C* **2014,** *118* (23), 12325-12332.

(S5) Tian, J.; Hustad, P. D.; Coates, G. W. A new catalyst for highly syndiospecific living olefin polymerization: Homopolymers and block copolymers from ethylene and propylene. *J. Am. Chem. Soc.* **2001,** *123* (21), 5134-5135.

(S6) Schindelin, J.; Arganda-Carreras, I.; Frise, E.; Kaynig, V.; Longair, M.; Pietzsch, T.; Preibisch, S.; Rueden, C.; Saalfeld, S.; Schmid, B.et al. Fiji: an open-source platform for biological-image analysis. *Nat. Methods* **2012,** *9*, 676.

(S7) Rueden, C. T.; Schindelin, J.; Hiner, M. C.; DeZonia, B. E.; Walter, A. E.; Arena, E. T.; Eliceiri, K. W. ImageJ2: ImageJ for the next generation of scientific image data. *BMC Bioinf.* **2017,** *18* (1), 529-529.

(S8) Linkert, M.; Rueden, C. T.; Allan, C.; Burel, J.-M.; Moore, W.; Patterson, A.; Loranger, B.; Moore, J.; Neves, C.; MacDonald, D.et al. Metadata matters: Access to image data in the real world. *J. Cell Biol.* **2010,** *189* (5), 777-782.

(S9) Perez, F.; Granger, B. E. IPython: A system for interactive scientific computing. *Comput. Sci. Eng.* **2007,** *9* (3), 21-29.

(S10) Walt, S. v. d.; Colbert, S. C.; Varoquaux, G. The NumPy array: A structure for efficient numerical computation. *Comput. Sci. Eng.* **2011,** *13* (2), 22-30.

(S11) Hunter, J. D. Matplotlib: A 2D graphics environment. *Comput. Sci. Eng.* **2007,** *9* (3), 90-95.

(S12) Delferro, M.; McInnis, J. P.; Marks, T. J. Ethylene Polymerization Characteristics of an Electron-Deficient Nickel(II) Phenoxyiminato Catalyst Modulated by Non-Innocent Intramolecular Hydrogen Bonding. *Organometallics* **2010,** *29* (21), 5040-5049.

(S13) Shu, D.; Mouat, A. R.; Stephenson, C. J.; Invergo, A. M.; Delferro, M.; Marks, T. J. Ligand-Unsymmetrical Phenoxyiminato Dinickel Catalyst for High Molecular Weight Long-Chain Branched Polyethylenes. *ACS Macro Lett.* **2015,** *4* (11), 1297-1301.

(S14) Kresse, G.; Hafner, J. Ab initio molecular dynamics for liquid metals. *Phys. Rev. B* **1993,** *47* (1), 558-561.

(SS16) Kresse, G.; Furthmüller, J. Efficient iterative schemes for ab initio total-energy calculations using a plane-wave basis set. *Phys. Rev. B* **1996,** *54* (16), 11169-11186.

(S17) Kresse, G.; Furthmüller, J. Efficiency of ab-initio total energy calculations for metals and semiconductors using a plane-wave basis set. *Comput. Mater. Sci.* **1996,** *6* (1), 15-50.

(S18) Blöchl, P. E. Projector augmented-wave method. *Phys. Rev. B* **1994,** *50* (24), 17953-17979.

(S19) Kresse, G.; Joubert, D. From ultrasoft pseudopotentials to the projector augmented-wave method. *Phys. Rev. B* **1999,** *59* (3), 1758-1775.

S(20) Sun, J.; Ruzsinszky, A.; Perdew, J. P. Strongly constrained and appropriately normed semilocal density functional. *Phys. Rev. Lett.* **2015,** *115* (3), 036402.
(S21) Sabatini, R.; Gorni, T.; de Gironcoli, S. Nonlocal van der Waals density functional made simple and efficient. *Phys. Rev. B* **2013,** *87* (4), 041108.
(S22) Monkhorst, H. J.; Pack, J. D. Special points for Brillouin-zone integrations. *Phys. Rev. B* **1976,** *13* (12), 5188-5192.
(S23) Makov, G.; Payne, M. C. Periodic boundary conditions in ab initio calculations. *Phys. Rev. B* **1995,** *51* (7), 4014-4022.
(S24) Harris, J. Simplified method for calculating the energy of weakly interacting fragments. *Phys. Rev. B* **1985,** *31* (4), 1770-1779.
(S25) Kienzle, D. M.; Becerra-Toledo, A. E.; Marks, L. D. Vacant-site octahedral tilings on $SrTiO_3$ (001), the ($\sqrt{13}$ x $\sqrt{13}$)*R*33.7^o surface, and related structures. *Phys. Rev. Lett.* **2011,** *106* (17), 176102.
(S26) Newell, D.; Harrison, A.; Silly, F.; Castell, M. $SrTiO_3$(001)-($\sqrt{5}$x$\sqrt{5}$)-*R*26.6^o reconstruction: A surface resulting from phase separation in a reducing environment. *Phys. Rev. B* **2007,** *75* (20), 205429.